

Cite this: *Sustainable Food Technol.*,
2026, 4, 2099

Microencapsulation of kratom leaf extract *via* spray drying: impact of inlet temperature and wall materials on stability and shelf life

Supanit Khongtongsang,^a Mohammad Fikry,^{ab} Saeid Jafari,^a Sochannet Chheng,^{id ac} Isaya Kijpatanasilp^a and Kitipong Assatarakul^{id *a}

Microencapsulation offers a sustainable approach to improve the stability, functionality, and shelf life of bioactive compounds in food systems, reducing product waste and enhancing resource efficiency. The objectives of this study were to microencapsulate kratom leaf extract (KLE) using spray drying with gum arabic (GA) and resistant maltodextrin (RMD) at two inlet temperatures (150 and 160 °C), to evaluate the resulting microcapsules in terms of their physicochemical properties and assess bioactive retention, specifically total phenolic and flavonoid contents, as well as antioxidant activity, and to investigate stability and shelf-life prediction using kinetic modeling. The resulting microcapsules were evaluated for physicochemical properties, bioactive retention, antioxidant activity, and storage stability. Encapsulation yield ranged from 45.3–62.7%, while encapsulation efficiency ranged from 70.8–83.5%, with GA at 160 °C showing the highest performance. Moisture content remained within the range of 2.1–3.6%, and solubility ranged from 82.4–92.1%, with RMD providing greater solubility and lower residual moisture. Total phenolic content retention ranged from 65.2–79.6%, while total flavonoid content retention ranged from 61.4–76.8%. Antioxidant activity (DPPH inhibition) decreased by approximately 20% during processing, with GA at 160 °C preserving the highest activity. Storage studies showed that water activity remained below the stability threshold ($a_w = 0.30$), and first-order kinetic modeling predicted a shelf-life extension of up to 90 days under ambient conditions. Morphological analysis revealed spherical particles with smooth surfaces at 160 °C, whereas higher temperatures induced surface collapse and shrinkage. Overall, GA provided superior protection of phenolics and antioxidants, while RMD enhanced solubility and reduced residual moisture. The findings highlight the potential of using food-grade wall materials and optimized spray drying conditions for scalable production of stable KLE microcapsules suitable for functional food and nutraceutical applications.

Received 3rd October 2025
Accepted 13th November 2025

DOI: 10.1039/d5fb00648a

rsc.li/susfoodtech

Sustainability spotlight

This study highlights a sustainable microencapsulation approach using plant-based, biodegradable wall materials (gum arabic and resistant maltodextrin) to enhance the shelf life and stability of kratom leaf extract. By optimizing spray drying conditions, the process achieves efficient bioactive preservation through low-energy input and minimal resource use. The findings promote reduced food waste, extended product usability, and environmentally responsible formulation practices, supporting the advancement of green technologies in functional food and nutraceutical production.

1 Introduction

Kratom (*Mitragyna Speciosa*) is a tropical plant belonging to the Rubiaceae family and is indigenous to Southeast Asia.¹ For hundreds of years, kratom has been utilized in various regions

of Thailand and is known by several local names, including Thom, E-Thang, Ketum, Kratum-Koke, and Maeng Da Leaf.² Traditionally, fresh kratom leaves are commonly chewed or boiled to create a decoction. In contrast, dried leaves are typically smoked, brewed into tea, or consumed as an herbal drink, often with added honey and lemon.³ Kratom has historically been used to relieve muscle fatigue and tiredness and as an herbal remedy for various common ailments, including diarrhea, diabetes, coughing, and hypertension. Additionally, it has been employed as an alternative to morphine or opium for treating drug addiction.⁴ Some studies have shown that kratom exhibits a range of biological activities, such as anti-

^aDepartment of Food Technology, Faculty of Science, Chulalongkorn University, 10330, Bangkok, Thailand. E-mail: Kitipong.A@chula.ac.th; Tel: +66-2218-5328

^bDepartment of Agricultural and Biosystems Engineering, Faculty of Agriculture, Benha University, Moshtohor, Toukh, 13736, Egypt

^cDepartment of Food Chemical Engineering, Kampong Speu Institute of Technology, Kampong Speu 050601, Cambodia



inflammatory, antinociceptive, antioxidant, and antimicrobial properties.⁵ For these reasons, kratom leaves hold significant economic value, with fresh leaves selling for \$8 to \$10 per kilogram in Thai markets as of 2022.⁶

Extracting bioactive compounds from kratom leaves can enhance both the commercial value of the raw material and the profitability of its processing. Consequently, kratom leaves have garnered significant attention from researchers exploring both traditional and novel extraction techniques.^{7–10} However, the stability of these extracted compounds can be compromised during processing and storage due to factors such as solvents, pH, temperature, oxygen, light, and enzymes.¹¹ Hence, finding alternative methods to enhance the stability of these bioactive compounds during processing and storage is crucial.

The stabilization of bioactive compounds can be enhanced using microencapsulation technologies, such as spray drying,¹² to improve their suitability for industrial applications and ensure their bioavailability. Spray drying is the preferred method for microencapsulation due to its cost-effectiveness, user-friendliness, and its ability to produce high-quality particles.¹³

Spray drying microencapsulation is a technique used to protect essential substances from unwanted decomposition or reactions during storage.¹⁴ This technology involves embedding active ingredients within microparticle matrices, creating a physical barrier between the active compound and the external environment while regulating its release. By encapsulating a bioactive compound in a biopolymer, the process shields it from oxygen, moisture, and other environmental factors, thus enhancing its stability. Additionally, it converts liquid solutions into powders, making them easier to handle.¹⁵

Various encapsulating agents are employed in spray drying, including polysaccharides (such as starch, resistant maltodextrin (RMD), corn syrups, and gum arabic (GA)), lipids (like stearic acid and mono- and diglycerides), and proteins (including gelatin, casein, milk serum, soy, and wheat). These substances are favored for their high-water solubility, low viscosity, neutral taste, and colorless solutions, making them widely utilized in the food industry (Jafari *et al.*, 2023).¹³

On the other hand, using mathematical models is a highly effective approach to assess quality parameters at various stages of processing. Zero-order and first-order equations are frequently utilized to describe the changes in quality properties over time. Predictive models have been previously developed to evaluate the shelf life of various products by integrating the physical and phytochemical indicators.¹⁶

Bioactive compounds from different plant leaves have been previously microencapsulated using spray drying technology.^{12,14,17–23}

Although kratom (*Mitragyna speciosa*) has been studied for its phytochemical composition and potential bioactivity,^{10,24–26} no previous reports have investigated its microencapsulation using spray drying. Microencapsulation is crucial for protecting kratom extract from degradation, improving stability, and facilitating reconstitution into functional products. However, knowledge remains limited regarding how different wall materials and processing conditions influence these outcomes.

Therefore, the objectives of this study were to microencapsulate kratom leaf extract (KLE) using spray drying with gum arabic (GA) and resistant maltodextrin (RMD) at two inlet temperatures (150 and 160 °C), to characterize the resulting microcapsules in terms of their physicochemical properties, to evaluate bioactive retention including total phenolic and flavonoid contents as well as antioxidant activity, and to assess shelf-life using kinetic modeling.

2 Materials and methods

2.1. Preparation of kratom leaf extract (KLE)

Kratom leaves were sourced from a domestic market in Bangkok, Thailand. They were first rinsed with water to eliminate dirt, and then dried in a lab oven (Memmert, DO 6062, Germany) at a temperature of 60 °C until their moisture content (MC) was reduced to less than 5%. The dried leaves were then ground and passed through a 50-mesh sieve.

For preparing kratom leaf extract (KLE), three grams of the powdered leaves were dissolved in 120 mL of solvent, following the modified procedures of ref. 27. Ultrasonic-assisted extraction was performed using an ultrasonic homogenizer (UP400S Ultrasonic processor, Hielscher, Germany). The ultrasonic settings were as follows: 400 W, 50% amplitude, 7 mm tip, pulse 30 s on/10 s off, 250 mL beaker, 50% immersion, and ice bath ($T < 40$ °C). Vacuum evaporation was also conducted at 40 °C under 100 mbar pressure until the extract reached a total solids content of approximately 15–20% (w/v), measured gravimetrically. Feasibility for encapsulation was confirmed by viscosity (< 50 mPa s at 25 °C) and absence of precipitation, ensuring stable feed for spray drying. Based on preliminary experiments, the optimum extraction conditions included 90% (v/v) ethanol concentration, 30-min extraction time, and an extraction ratio of 1 : 40 (w/v). According to the method described in ref. 28, the extracts were centrifuged at $6000 \times g$ (rotor radius 10 cm) for 15 min at 25 °C using a centrifuge (Centrifuge Kubota, series 6000, Japan). The supernatant was filtered using Whatman No. 1 paper in order to eliminate coarse particles and then subjected to vacuum evaporation process utilizing a rotary evaporator (Oilbath B-485, BÜCHI, Switzerland) to ~20% solids (w/w). The samples were stored in amber vials at 4 °C for subsequent analysis.

2.2. Spray drying microencapsulation process

Microencapsulation was carried out using resistant maltodextrin (RMD; Fibersol-2, Matsutani, Japan), gum arabic (GA; Agrigum, UK), and their combination as coating materials. Concentrations (w/w) were selected based on preliminary trials to achieve comparable feed viscosities (~20–40 mPa s) while remaining within solubility limits: 20% for GA (to avoid excessive viscosity), 40% for RMD (optimal solubility), and a 1 : 1 blend (40% RMD with 20% GA) at equivalent total solids for comparison. All formulations were spray dried at inlet temperatures of 150 and 160 °C using a KLE-to-coating material ratio of 1 : 2 (w/w). The mixtures were prepared by combining KLE with the coating materials (Table 1) and stirring continuously with



Table 1 Production conditions of KLE microcapsules using spray drying

Experiment	Inlet temperature	Type of coating material	KLE to coating material ratio (w/w)
1	150 °C	40% resistant maltodextrin	1 : 2
2		20% gum arabic	1 : 2
3		40% resistant maltodextrin with 20% gum arabic (1 : 1 ratio)	1 : 2
4	160 °C	40% resistant maltodextrin	1 : 2
5		20% gum arabic	1 : 2
6		40% resistant maltodextrin with 20% gum arabic (1 : 1 ratio)	1 : 2

a magnetic stirrer (SCIOLOGEX, SCI550-S, USA) for 10 min. The mixture was then homogenized with a high-speed blender (Ystral, model X10, Germany) at 11 000 rpm for 10 min. The operating conditions were as follows: feed solids 20–40% w/w, viscosity 20–40 mPa s, pump 10 mL min⁻¹, aspirator 90%, atomizing air 0.7 mm nozzle at 1 bar, and feed temperature 25 °C. The resulting solutions were processed through a spray dryer (BUCHI, B-290, Switzerland) set at inlet temperatures of 150 and

160 °C and an outlet temperature ranging from 85–95 °C. The resulting powders were stored at –20 °C for analysis of their properties (e.g., encapsulation yield, encapsulation efficiency, moisture content, water activity, water solubility, TPC, TFC, TTC, and antioxidant activity *via* DPPH and FRAP) under different conditions. Fig. 1 reveals the production flow chart of KLE microcapsules of bioactive compounds extracted from kratom leaves.

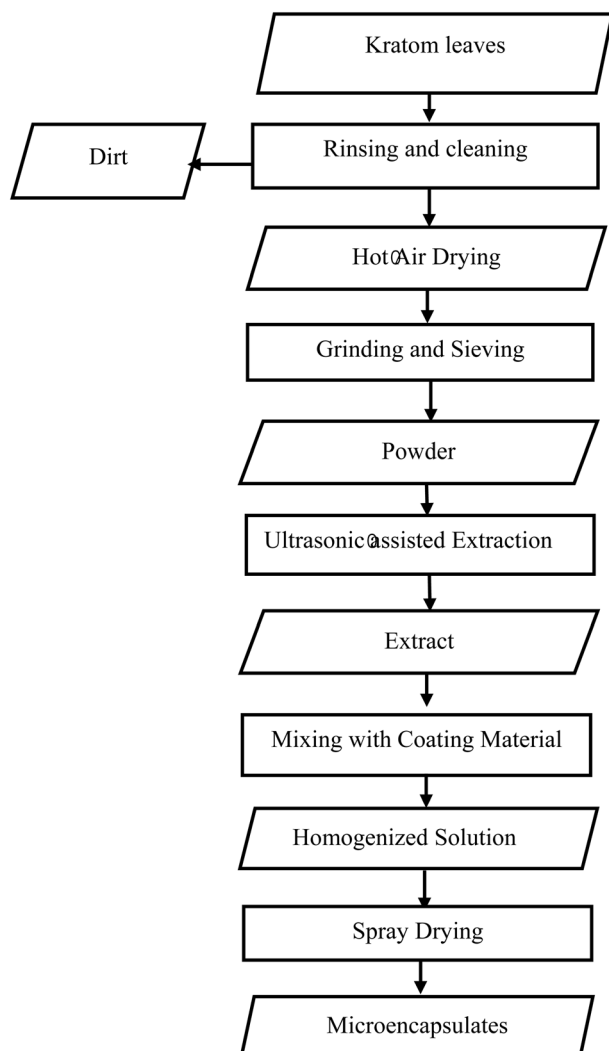


Fig. 1 Production flow chart of KLE microcapsules of bioactive compounds extracted from kratom leaves.

2.3. Calculation of the encapsulation yield and encapsulation efficiency

Following the procedure of ref. 29, the encapsulation yield (%) was determined and calculated using the following equation (eqn (1)):

$$\text{Encapsulation yield}(\%) = \frac{m_{\text{capsules, collected}}}{m_{\text{solids, initial}}} \times 100 \quad (1)$$

where $m_{\text{capsules, collected}}$ is the total mass of KLE microcapsules collected from the spray dryer and $m_{\text{solids, initial}}$ is the mass of total solids in the feed before drying.

To calculate the percentage of encapsulation efficiency, the total bioactive compound content was determined first. A sample of 0.1 g of KLE encapsulated powder was dissolved in 1 mL of a mixed solution (ethanol : acetic acid : water in a 50 : 8 : 42 ratio) and shaken with a vortex mixer for 1 min. The sample was then centrifuged at 10 000 rpm for 5 min and filtered. The total phenolic content was analyzed using Folin–Ciocalteu colorimetry as described in ref. 30. Next, to determine the surface bioactive compounds, 0.1 g of KLE encapsulated powder was dissolved in a mixed solution of ethanol and methanol (1 : 1 ratio) and shaken with a vortex mixer for 1 min. The sample was filtered, and the total phenolic content was again analyzed using Folin–Ciocalteu colorimetry.

The encapsulation efficiency (%) was calculated using the following formula (eqn (2)) according to ref. 31:

$$\text{EE} = [(T_{\text{O}} - S_{\text{O}})/T_{\text{O}}] \times 100 \quad (2)$$

where T_{O} represents the total bioactive compounds and S_{O} represents the surface bioactive compounds.

2.4. Determination of physical attributes of KLE microcapsules

2.4.1 Determination of moisture content and water activity. The moisture content of KLE microcapsules was



measured using an infrared moisture analyzer (MA35, Sartorius, Goettingen, Germany) according to the method described in ref. 32. Additionally, the water activity (a_w) at 25 °C was determined with an Aqua Lab instrument (AquaLab Pre, Decagon, QTEtech, Hanoi, Vietnam). The reported results are an average of three replicates.

2.4.2 Determination of color attributes. According to the method outlined in ref. 32, the color of KLE microcapsules was measured using a portable spectrophotometer (CM-600d, Konica Minolta, INC, Osaka, Japan) within the Lab system. The color values were expressed using the CIE $L^*a^*b^*$ system, where the brightness coordinate L^* indicates whiteness/darkness, the chromaticity coordinate a^* indicates redness/greenness, and the chromaticity coordinate b^* indicates yellowness/blueness. All measurements were taken in triplicate, and the mean values were recorded. The total color difference, ΔE , was subsequently calculated using the following formula (eqn (3)),

$$\Delta E = \sqrt{(L_i^* - L_t^*)^2 + (a_i^* - a_t^*)^2 + (b_i^* - b_t^*)^2} \quad (3)$$

where L_i^* , a_i^* , and b_i^* are the initial values for KLE microcapsules at zero days, and L_t^* , a_t^* , and b_t^* are the measured values at different storage times.

2.4.3 Determination of water solubility. The water solubility measurement was performed following the procedure outlined in ref. 33 involved adding 1 g of KLE microcapsules to 100 mL of distilled water, and then the mixture was stirred using a magnetic stirrer (SCIOLOGEX, model SCI550-S, USA) for 30 min. Afterward, the mixture was centrifuged (Centrifuge Kubota, series 6000, Japan) at 3000×g for 5 min. A 25 mL aliquot of the supernatant was transferred to a pre-weighed Petri dish and dried in an oven (Memmert, DO 6062, Germany) operated at a temperature of 105 °C for a period of 5 h (the aliquot was homogenized before drying). The solubility was estimated using the following formula (eqn (4)).

$$\text{Water solubility(\%)} = \frac{\text{Solid content in supernatant}}{\text{Total solid content}} \times 100 \quad (4)$$

2.5. Determination of phytochemical properties of KLE microcapsules

2.5.1 Measurements of total phenolic content (TPC). TPC of KLE microcapsules was measured using a modified approach based on ref. 34. Briefly, 1 g of the microencapsulated samples was added to 5 mL of distilled water, and then 0.5 mL of the Folin-Ciocalteu phenol reagent was added. The mixture was incubated for 8 min, afterward, 1.5 mL of 20% Na_2CO_3 was added, and the mixture was left at 25 °C for 20 min (calibration: 0–200 mg GAE per L, $R^2 = 0.994$; samples diluted to 0.2–0.8 AU). A UV-vis spectrophotometer (Eppendorf BioSpectrometer® basic, Thailand) was utilized to measure the absorbance of the sample at 765 nm, using a blank for reference, according to ref. 27; gallic acid was used as the standard for the calibration curve ($Y = 4.83X + 0.0792$, $R^2 = 0.994$). TPC was expressed as gallic acid equivalents (mg GAE per mL). Three independent extractions and encapsulations were carried out in triplicate, with each replicate measured three times; data are presented as mean \pm SD.

2.5.2 Analysis of total flavonoid content (TFC). To assess TFC, 1 mL of the microencapsulated solution was added to 1 mL of 2% w/v aluminum chloride in methanol and incubated for 30 min. A UV-vis spectrophotometer (Eppendorf BioSpectrometer® basic, Thailand) equipped with a cuvette was used to measure the absorbance at 430 nm using a blank for reference.³⁵ TFC (mg QE per mL) was calculated based on the quercetin calibration curve ($Y = 0.8986X + 0.024$, $R^2 = 0.995$). Three independent extractions and encapsulations were carried out in triplicate, with each replicate measured three times; data are presented as mean \pm SD.

2.5.3 Determination of antioxidant activity by DPPH scavenging activity. Following a slightly modified version of the procedure used in ref. 36 and 37, the 2,2-diphenyl-1-picrylhydrazyl (DPPH) assay was performed to evaluate the antioxidant activity of KLE microcapsules. A 0.2 mL of aqueous extract (from 1 g powder in 10 mL water, consistent with TPC extraction for comparability) was added to 2 mL of methanol and 2 mL of the DPPH solution. The mixture was incubated for 30 min at 25 °C in the dark. Following incubation, a UV-vis spectrophotometer (Eppendorf BioSpectrometer® basic, Thailand) was used to determine the absorbance at 517 nm. Methanol served as the blank and the values of antioxidant activity of KLE microcapsules were then computed using the specified equation (eqn (5)). Antioxidant activity was quantified against a Trolox calibration curve (0–1000 μM ; $R^2 = 0.993$) for DPPH.

2.5.4 Determination of antioxidant activity by ferric reducing antioxidant power (FRAP) assay. To determine the FRAP antioxidant activity of KLE microcapsules, 1 g of KLE microcapsules was dissolved in 10 mL of distilled water and thoroughly mixed using a vortex mixer for 3 min. The sample was placed in a hot tub, maintaining a shaking temperature of 30 °C for up to 30 min. Next, the sample was subjected to centrifugation at 4000 rpm for 20 min.³¹ Then, 2.85 mL of FRAP solution was mixed with 0.15 mL of the sample. The FRAP solution was prepared by combining acetate buffer (300 mM, pH = 3.6), 20 mM FeCl_3 , and TPTZ solution (prepared in 40 mM HCl) in a ratio of 10 : 1 : 1 and warming it to 37.5 °C before use. After the sample and FRAP solution were thoroughly mixed, the mixture was incubated for 30 min. Antioxidant activity was quantified against a Trolox calibration curve (0–1000 μM ; $R^2 = 0.991$) for FRAP. The absorbance was measured at 593 nm.³⁸ The DPPH and FRAP inhibition were calculated using the following formula (eqn (5)):

$$\% \text{Inhibition} = \left[1 - \frac{A_{\text{sample}}}{A_{\text{control}}} \right] \times 100 \quad (5)$$

where A_{control} denotes the mixture of methanol and DPPH solution and A_{sample} refers to the mixture of the extract and DPPH/FRAP solution.

2.5.5 Determination of total tannin content (TTC). The tannin content in KLE microcapsules was assessed using a method adapted from ref. 39. In summary, 500 μL of the extract (from 0.1 g of KLE microcapsules in 1 mL water) were incubated with 10 mg polyvinylpyrrolidone (PVPP) (to bind tannins) or without (replaced by water as control) for 15 min at 4 °C, followed by centrifugation at 15 000×g for 10 min. The



supernatants were then analysed using the total phenolic content (TPC) assay. The tannin content was calculated based on the difference in TPC values between the PVPP-treated and water-treated samples. Tannic acid ($0\text{--}100\ \mu\text{g mL}^{-1}$) served as the standard, and tannin levels were reported as mg TAE per 100 mL.

2.5.6 Mitragynine quantification by HPLC. Mitragynine content in KLE microcapsules was quantified using high-performance liquid chromatography (HPLC) with UV detection. Approximately 100 mg of encapsulated powder was extracted with 10 mL of methanol containing 0.1% formic acid, vortexed for 1 min, sonicated for 15 min at ambient temperature, and centrifuged (5000 g, 10 min). The supernatant was diluted as needed, filtered through a $0.22\ \mu\text{m}$ PTFE syringe filter, and transferred to vials. Chromatographic analysis was performed on a C18 column ($150 \times 4.6\ \text{mm}$, $5\ \mu\text{m}$; $35\ ^\circ\text{C}$) using a binary gradient system consisting of water with 0.1% formic acid (solvent A) and acetonitrile with 0.1% formic acid (solvent B). The gradient program was set as follows: 35% B (0 min) \rightarrow 55% B (6 min) \rightarrow 70% B (10 min, held to 12 min) \rightarrow 35% B (12.1 min, re-equilibrated to 20 min) with a flow rate of $1.0\ \text{mL min}^{-1}$, injection volume of $10\ \mu\text{L}$, and detection wavelength of 225 nm. Calibration curves were prepared using mitragynine standard solutions ($0.05\text{--}50\ \mu\text{g mL}^{-1}$), yielding linearity with $R^2 \geq 0.999$. Method performance was validated with a limit of quantification (LOQ) of $0.05\ \mu\text{g mL}^{-1}$, precision (RSD) $\leq 5\%$, and recovery of 90–110% from spiked matrix samples. Mitragynine concentrations were expressed as mg per g dry basis, corrected for residual moisture.

2.6. Assessment of morphology of KLE microcapsules

To assess the microstructure of KLE microcapsules, the appearance of the microcapsules was examined using a scanning electron microscope (SEM) and an energy dispersive X-ray spectrometer (JEOL, JSM-IT300 Oxford, X-Max N 20) with a 15 kV magnification at $1000\times$, $3000\times$, and $5000\times$. The samples were sputter-coated with gold (10 nm thickness) under vacuum before imaging.

2.7. Investigation of storage stability of KLE microcapsules

Formulations were selected using a multi-criteria optimization approach that considered lowest MC/a_w and highest TPC, TFC, and antioxidant activity. Weighted scoring was applied (40% bioactive retention, 30% physical stability, and 30% solubility), with the GA@160 $^\circ\text{C}$ formulation achieving the highest score (85/100). Ten grams of KLE microcapsules, encapsulated using gum arabic and processed *via* spray drying at 160 $^\circ\text{C}$, were packaged in laminated aluminum foil bags and stored under vacuum at room temperature ($30 \pm 5\ ^\circ\text{C}$). Quality properties were monitored every 15 days over a period of 90 days to assess changes.

2.8. Kinetic modelling of changes in characteristics of KLE microcapsules

To estimate the reaction order of the alterations in various characteristics of KLE microcapsules, the experimental data were analysed using eqn (6). Zero-order and first-order

equations, which are frequently employed to model reactions associated with food quality deterioration, were derived from eqn (6) and are represented in eqn (7) and (8).

$$-\frac{dc}{dt} = kC^n \quad (6)$$

$$C = C_o \pm kt \quad (7)$$

$$\ln C = \ln C_o \pm kt \quad (8)$$

In the given equations, C and C_o denote the property value at a specific time and the initial value, respectively, while “ t ” indicates the storage duration. The parameter “ k ” is the reaction rate constant (per day) and “ n ” represents the reaction order of the changes. The symbols (+) and (–) indicate the increase and decrease in attributes, respectively.

2.9. Predicting the shelf life by integration of the quality properties

Shelf-life was estimated based on the minimum time to first failure among key physicochemical and phytochemical attributes, namely moisture content (MC), water activity (a_w), total phenolic content (TPC), total flavonoid content (TFC), total tannin content (TTC), antioxidant activity by DPPH radical scavenging, and ferric reducing antioxidant power (FRAP).

For each parameter, a threshold value was defined to indicate the point of quality loss. Specifically, the water activity threshold was set at 0.30, as values above this level promote chemical reactions and increase the risk of microbial growth.^{40,41} For antioxidant stability, shelf-life termination was determined when DPPH radical scavenging activity decreased by 20% relative to the initial value, which was considered a critical limit for functional quality retention.

A least-squares fitting procedure was employed to ascertain the kinetic order by adjusting the experimental data to solve the general expression of eqn (6). The kinetic parameters derived for each attribute were then used to estimate the shelf life of KLE microcapsules using eqn (9), as demonstrated in prior studies in ref. 16.

$$\text{Shelf life}(\text{day}) = \frac{C - C_o}{k} \quad (9)$$

2.10. Statistical analysis

Data were analyzed using two-way analysis of variance (ANOVA) to evaluate the effects of wall materials and drying temperature on the properties of KLE microcapsules, and mean comparisons were performed using Tukey's HSD test at a significance level of $p \leq 0.05$. Significant differences among wall materials are denoted by uppercase letters, while differences among temperatures are indicated by lowercase letters. Effect sizes were also computed to investigate the importance of each factor. Moreover, regression analysis was performed to evaluate the precision of the models in representing the observed data. The selection of the best model was based on achieving the highest correlation coefficient, $R^2 \geq 0.90$, as recommended by previous studies.⁴² Data analysis and modelling were carried out



using Minitab v. 18 (Minitab Inc., State College, PA, USA). The proportion of variance explained by each factor was expressed as eta-squared (η^2) values obtained from the ANOVA, indicating the relative effect size of the wall material, inlet temperature, and their interaction.

3 Results and discussion

3.1 Encapsulation yield of KLE microcapsules

The two-way ANOVA results revealed the significant main and interaction effects of wall materials and temperature on encapsulation yield. The encapsulation yield ranged from 58.2 to 72.9%, with wall materials exerting a moderate effect ($\eta^2 = 0.28$). Resistant maltodextrin (RMD) generally produced higher recovery values compared to gum arabic (GA), underscoring the importance of carrier selection in determining encapsulation efficiency. In contrast, temperature exhibited only a small effect ($\eta^2 = 0.07$), suggesting that drying conditions had a limited influence on yield relative to wall material composition, as illustrated in Table 2. Higher excipient concentrations in RMD and blend experiments contributed to reduced wall adhesion, enhancing yield. The low yield for gum arabic is attributed to its pseudoplastic nature at high concentrations (20% in this study), which increases viscosity⁴³ and causes it to adhere to the inner surfaces of the spray dryer, reducing yield. Additionally, increasing the spray drying temperature from 150 °C to 160 °C significantly ($p \leq 0.05$) improved the yield when using gum arabic as the coating material. Higher temperatures enhance thermal energy, breaking intermolecular bonds, which reduces viscosity and adhesion to the spray dryer surfaces.⁴⁴

Conversely, using resistant maltodextrin alone or in combination with gum arabic resulted in lower yields at higher spray drying temperatures. This is likely due to heat accumulation causing the microcapsules to melt and stick to the inner surfaces of the spray dryer, thereby decreasing the overall yield.

3.2 Encapsulation efficiency of KLE microcapsules

The results presented in Table 2, revealed that the values of encapsulation efficiency (EE), ranged from 68.3% to 92.7%, with both the wall material and temperature exerting strong influences ($\eta^2 = 0.32$ and 0.18 , respectively), alongside a significant interaction effect ($\eta^2 = 0.11$). Similarly, hygroscopicity (HG), which varied between 7.2% and 12.5%, was markedly influenced by the wall material ($\eta^2 = 0.26$) and temperature ($\eta^2 = 0.14$), with an additional moderate interaction ($\eta^2 = 0.09$). The use of gum arabic as a coating material at an inlet spray drying temperature of 160 °C resulted in the highest encapsulation efficiency, while resistant maltodextrin at the same temperature resulted in the lowest efficiency. The emulsion properties of gum arabic enable it to form a better encapsulating film compared to resistant maltodextrin, resulting in higher encapsulation efficiency in microcapsules coated with gum arabic.⁴⁵

Considering the inlet spray drying temperature, higher temperatures led to more effective water evaporation from the particles, thus increasing encapsulation efficiency. However, excessively high temperatures might damage the

microcapsules, exposing the core material to direct heat and potentially degrading the active compounds.⁴⁶ Consequently, microcapsules using resistant maltodextrin and a combination of resistant maltodextrin with gum arabic exhibited reduced encapsulation efficiency when the inlet spray drying temperature increased to 160 °C. In general, encapsulation efficiency values were benchmarked against the initial TPC in the crude extract (45.2 ± 2.1 mg GAE per mL), indicating 82–92% retention post-encapsulation and thereby confirming effective protection.

3.3 Moisture content (%) and water activity (a_w) of KLE microcapsules

The study examined the moisture content and water activity of KLE microcapsules produced through spray drying, varying the types of coating materials and two inlet drying temperatures (Table 2). Moisture content ranged from 2.6 to 6.8%, and was more strongly affected by temperature ($\eta^2 = 0.27$) than the wall material ($\eta^2 = 0.15$). Higher inlet temperature reduced moisture in GA samples but slightly increased it in RMD powders, suggesting carrier-dependent responses to drying kinetics. It was found that microcapsules with gum arabic as the coating material had higher moisture content compared to those using resistant maltodextrin. This is because gum arabic, a complex heteropolysaccharide, is hydrophilic, enabling it to retain more moisture than resistant maltodextrin. Maintaining low water activity or moisture content increases the glass transition temperature (T_g), and storage at temperatures below T_g (~ 50 °C for GA/RMD) ensures glassy-state stability.⁴⁷

When the inlet spray drying temperature was increased from 150 °C to 160 °C, the moisture content of microcapsules with gum arabic decreased, as the higher temperature facilitated better water evaporation.⁴⁸ GA exhibits higher viscosity at lower temperatures, which can trap moisture; at elevated temperatures, viscosity decreases, facilitating evaporation. In contrast, RMD is inherently less viscous and less affected by this behavior. In contrast, microcapsules with resistant maltodextrin and those with a combination of gum arabic and resistant maltodextrin showed an increase in moisture content ($3.52 \pm 0.1\%$ and $3.34 \pm 0.2\%$, respectively) at higher temperatures (Table 2). Higher temperatures generate a steeper heat gradient, enhancing moisture diffusion in RMD but leading to tackiness in the blends (Tay *et al.*, 2021).⁴⁹

Clearly from Table 2, it can be observed that water activity (a_w) values were low (0.16–0.26), indicating suitability for storage stability. Both factors had small effects ($\eta^2 \leq 0.12$), indicating robustness across treatments, which are within the standard reference values for food powders that should not exceed a water activity of 0.3. Water activity (a_w) is more closely associated with bound water; GA's hydrophilic nature tightly binds water, which maintains low a_w values even at higher total moisture content.⁵⁰

3.4 Water solubility of KLE microcapsules

Water solubility was consistently high (91.8–95.6%), with significant though smaller effects of the carrier ($\eta^2 = 0.22$) and



Table 2 Mean values of physicochemical properties of kratom leaf extract microcapsules as affected by different wall materials and inlet temperatures^a

Properties	Inlet temperature (°C)	40% resistant maltodextrin	20% gum arabic	40% resistant maltodextrin + 20% gum arabic (1 : 1)	Carrier η^2	Temperature η^2	Interaction η^2																																																																																																																																																								
Yield (%)	150	72.85 ± 1.08Aa	58.24 ± 0.60Aa	67.52 ± 0.83Aa	0.28	0.07	0.05																																																																																																																																																								
	160	63.61 ± 3.81Aa	65.23 ± 3.54Aa	66.26 ± 0.98Aa				EE (%)	150	79.34 ± 2.88ABa	67.87 ± 1.50Aa	67.52 ± 0.89Aa	0.35	0.18	0.09	160	59.16 ± 5.26ABa	84.65 ± 1.32Aa	62.45 ± 2.53Aa	Water solubility (%)	150	95.55 ± 0.26Ba	91.82 ± 0.09Aa	93.21 ± 0.26Aa	0.22	0.1	0.04	160	95.34 ± 0.58Bb	95.10 ± 0.48Ab	94.75 ± 0.38Ab	Moisture content (%)	150	2.59 ± 0.09Aa	6.81 ± 0.15Aa	2.90 ± 0.07Aa	0.15	0.27	0.07	160	3.52 ± 0.07Aa	2.67 ± 0.10Aa	3.30 ± 0.13Aa	Water activity	150	0.23 ± 0.00Aa	0.26 ± 0.04Aa	0.18 ± 0.22Aa	0.08	0.12	0.03	160	0.21 ± 0.01Aa	0.16 ± 0.03Aa	0.22 ± 0.02Aa	<i>L</i> -Value*	150	64.32 ± 1.19Ca	60.76 ± 0.88Aa	62.80 ± 0.85Ba	0.19	0.14	0.06	160	64.80 ± 1.24Cb	60.41 ± 1.12Aa	63.05 ± 0.67Bb	<i>a</i> -Value*	150	-1.29 ± 0.02Db	-0.44 ± 0.06Aa	-0.51 ± 0.07Ba	0.24	0.1	0.05	160	-1.24 ± 0.01Da	-0.47 ± 0.04Aa	-0.63 ± 0.08Ca	<i>b</i> -Value*	150	4.07 ± 0.12Aa	7.62 ± 0.34Bb	6.67 ± 0.76Db	0.32	0.12	0.08	160	4.17 ± 0.87Aa	8.09 ± 0.83 Bc	8.25 ± 0.43 Dc	TPC	150	13.07 ± 2.13Ba	25.91 ± 1.45Aa	17.14 ± 0.30Aa	0.29	0.16	0.1	160	15.71 ± 0.65Ba	34.75 ± 2.66Aa	25.62 ± 2.21Aa	TTC	150	13.39 ± 2.34Aa	27.59 ± 1.58 a	17.11 ± 0.63Aa	0.25	0.2	0.12	160	18.66 ± 1.41Ab	35.46 ± 2.87 b	26.07 ± 1.50Ab	TFC	150	1.79 ± 0.20Ca	4.84 ± 0.50Aa	2.92 ± 0.23Ca	0.3	0.14	0.09	160	1.98 ± 0.40Ca	5.05 ± 0.06Aa	3.18 ± 0.23Ca	DPPH	150	243.54 ± 4.10Ca	279.93 ± 1.64Aa	233.54 ± 3.09Ca	0.27	0.18	0.08	160	239.72 ± 6.05Ca	305.24 ± 2.59Aa	238.78 ± 1.11Ca	FRAP	150	343.56 ± 3.12Aa	400.52 ± 2.01Aa	413.99 ± 2.33Aa	0.33	0.21	0.11	160	322.29 ± 4.59Aa	522.74 ± 2.47Aa	317.48 ± 8.14Aa	Mitragynine	150	0.96 ± 0.09Ca	1.89 ± 0.06Aa	1.36 ± 0.09Ca	0.21	0.09	0.05
EE (%)	150	79.34 ± 2.88ABa	67.87 ± 1.50Aa	67.52 ± 0.89Aa	0.35	0.18	0.09																																																																																																																																																								
	160	59.16 ± 5.26ABa	84.65 ± 1.32Aa	62.45 ± 2.53Aa				Water solubility (%)	150	95.55 ± 0.26Ba	91.82 ± 0.09Aa	93.21 ± 0.26Aa	0.22	0.1	0.04	160	95.34 ± 0.58Bb	95.10 ± 0.48Ab	94.75 ± 0.38Ab	Moisture content (%)	150	2.59 ± 0.09Aa	6.81 ± 0.15Aa	2.90 ± 0.07Aa	0.15	0.27	0.07	160	3.52 ± 0.07Aa	2.67 ± 0.10Aa	3.30 ± 0.13Aa	Water activity	150	0.23 ± 0.00Aa	0.26 ± 0.04Aa	0.18 ± 0.22Aa	0.08	0.12	0.03	160	0.21 ± 0.01Aa	0.16 ± 0.03Aa	0.22 ± 0.02Aa	<i>L</i> -Value*	150	64.32 ± 1.19Ca	60.76 ± 0.88Aa	62.80 ± 0.85Ba	0.19	0.14	0.06	160	64.80 ± 1.24Cb	60.41 ± 1.12Aa	63.05 ± 0.67Bb	<i>a</i> -Value*	150	-1.29 ± 0.02Db	-0.44 ± 0.06Aa	-0.51 ± 0.07Ba	0.24	0.1	0.05	160	-1.24 ± 0.01Da	-0.47 ± 0.04Aa	-0.63 ± 0.08Ca	<i>b</i> -Value*	150	4.07 ± 0.12Aa	7.62 ± 0.34Bb	6.67 ± 0.76Db	0.32	0.12	0.08	160	4.17 ± 0.87Aa	8.09 ± 0.83 Bc	8.25 ± 0.43 Dc	TPC	150	13.07 ± 2.13Ba	25.91 ± 1.45Aa	17.14 ± 0.30Aa	0.29	0.16	0.1	160	15.71 ± 0.65Ba	34.75 ± 2.66Aa	25.62 ± 2.21Aa	TTC	150	13.39 ± 2.34Aa	27.59 ± 1.58 a	17.11 ± 0.63Aa	0.25	0.2	0.12	160	18.66 ± 1.41Ab	35.46 ± 2.87 b	26.07 ± 1.50Ab	TFC	150	1.79 ± 0.20Ca	4.84 ± 0.50Aa	2.92 ± 0.23Ca	0.3	0.14	0.09	160	1.98 ± 0.40Ca	5.05 ± 0.06Aa	3.18 ± 0.23Ca	DPPH	150	243.54 ± 4.10Ca	279.93 ± 1.64Aa	233.54 ± 3.09Ca	0.27	0.18	0.08	160	239.72 ± 6.05Ca	305.24 ± 2.59Aa	238.78 ± 1.11Ca	FRAP	150	343.56 ± 3.12Aa	400.52 ± 2.01Aa	413.99 ± 2.33Aa	0.33	0.21	0.11	160	322.29 ± 4.59Aa	522.74 ± 2.47Aa	317.48 ± 8.14Aa	Mitragynine	150	0.96 ± 0.09Ca	1.89 ± 0.06Aa	1.36 ± 0.09Ca	0.21	0.09	0.05	160	1.06 ± 0.02Ca	1.96 ± 0.04Aa	1.38 ± 0.09Ca								
Water solubility (%)	150	95.55 ± 0.26Ba	91.82 ± 0.09Aa	93.21 ± 0.26Aa	0.22	0.1	0.04																																																																																																																																																								
	160	95.34 ± 0.58Bb	95.10 ± 0.48Ab	94.75 ± 0.38Ab				Moisture content (%)	150	2.59 ± 0.09Aa	6.81 ± 0.15Aa	2.90 ± 0.07Aa	0.15	0.27	0.07	160	3.52 ± 0.07Aa	2.67 ± 0.10Aa	3.30 ± 0.13Aa	Water activity	150	0.23 ± 0.00Aa	0.26 ± 0.04Aa	0.18 ± 0.22Aa	0.08	0.12	0.03	160	0.21 ± 0.01Aa	0.16 ± 0.03Aa	0.22 ± 0.02Aa	<i>L</i> -Value*	150	64.32 ± 1.19Ca	60.76 ± 0.88Aa	62.80 ± 0.85Ba	0.19	0.14	0.06	160	64.80 ± 1.24Cb	60.41 ± 1.12Aa	63.05 ± 0.67Bb	<i>a</i> -Value*	150	-1.29 ± 0.02Db	-0.44 ± 0.06Aa	-0.51 ± 0.07Ba	0.24	0.1	0.05	160	-1.24 ± 0.01Da	-0.47 ± 0.04Aa	-0.63 ± 0.08Ca	<i>b</i> -Value*	150	4.07 ± 0.12Aa	7.62 ± 0.34Bb	6.67 ± 0.76Db	0.32	0.12	0.08	160	4.17 ± 0.87Aa	8.09 ± 0.83 Bc	8.25 ± 0.43 Dc	TPC	150	13.07 ± 2.13Ba	25.91 ± 1.45Aa	17.14 ± 0.30Aa	0.29	0.16	0.1	160	15.71 ± 0.65Ba	34.75 ± 2.66Aa	25.62 ± 2.21Aa	TTC	150	13.39 ± 2.34Aa	27.59 ± 1.58 a	17.11 ± 0.63Aa	0.25	0.2	0.12	160	18.66 ± 1.41Ab	35.46 ± 2.87 b	26.07 ± 1.50Ab	TFC	150	1.79 ± 0.20Ca	4.84 ± 0.50Aa	2.92 ± 0.23Ca	0.3	0.14	0.09	160	1.98 ± 0.40Ca	5.05 ± 0.06Aa	3.18 ± 0.23Ca	DPPH	150	243.54 ± 4.10Ca	279.93 ± 1.64Aa	233.54 ± 3.09Ca	0.27	0.18	0.08	160	239.72 ± 6.05Ca	305.24 ± 2.59Aa	238.78 ± 1.11Ca	FRAP	150	343.56 ± 3.12Aa	400.52 ± 2.01Aa	413.99 ± 2.33Aa	0.33	0.21	0.11	160	322.29 ± 4.59Aa	522.74 ± 2.47Aa	317.48 ± 8.14Aa	Mitragynine	150	0.96 ± 0.09Ca	1.89 ± 0.06Aa	1.36 ± 0.09Ca	0.21	0.09	0.05	160	1.06 ± 0.02Ca	1.96 ± 0.04Aa	1.38 ± 0.09Ca																				
Moisture content (%)	150	2.59 ± 0.09Aa	6.81 ± 0.15Aa	2.90 ± 0.07Aa	0.15	0.27	0.07																																																																																																																																																								
	160	3.52 ± 0.07Aa	2.67 ± 0.10Aa	3.30 ± 0.13Aa				Water activity	150	0.23 ± 0.00Aa	0.26 ± 0.04Aa	0.18 ± 0.22Aa	0.08	0.12	0.03	160	0.21 ± 0.01Aa	0.16 ± 0.03Aa	0.22 ± 0.02Aa	<i>L</i> -Value*	150	64.32 ± 1.19Ca	60.76 ± 0.88Aa	62.80 ± 0.85Ba	0.19	0.14	0.06	160	64.80 ± 1.24Cb	60.41 ± 1.12Aa	63.05 ± 0.67Bb	<i>a</i> -Value*	150	-1.29 ± 0.02Db	-0.44 ± 0.06Aa	-0.51 ± 0.07Ba	0.24	0.1	0.05	160	-1.24 ± 0.01Da	-0.47 ± 0.04Aa	-0.63 ± 0.08Ca	<i>b</i> -Value*	150	4.07 ± 0.12Aa	7.62 ± 0.34Bb	6.67 ± 0.76Db	0.32	0.12	0.08	160	4.17 ± 0.87Aa	8.09 ± 0.83 Bc	8.25 ± 0.43 Dc	TPC	150	13.07 ± 2.13Ba	25.91 ± 1.45Aa	17.14 ± 0.30Aa	0.29	0.16	0.1	160	15.71 ± 0.65Ba	34.75 ± 2.66Aa	25.62 ± 2.21Aa	TTC	150	13.39 ± 2.34Aa	27.59 ± 1.58 a	17.11 ± 0.63Aa	0.25	0.2	0.12	160	18.66 ± 1.41Ab	35.46 ± 2.87 b	26.07 ± 1.50Ab	TFC	150	1.79 ± 0.20Ca	4.84 ± 0.50Aa	2.92 ± 0.23Ca	0.3	0.14	0.09	160	1.98 ± 0.40Ca	5.05 ± 0.06Aa	3.18 ± 0.23Ca	DPPH	150	243.54 ± 4.10Ca	279.93 ± 1.64Aa	233.54 ± 3.09Ca	0.27	0.18	0.08	160	239.72 ± 6.05Ca	305.24 ± 2.59Aa	238.78 ± 1.11Ca	FRAP	150	343.56 ± 3.12Aa	400.52 ± 2.01Aa	413.99 ± 2.33Aa	0.33	0.21	0.11	160	322.29 ± 4.59Aa	522.74 ± 2.47Aa	317.48 ± 8.14Aa	Mitragynine	150	0.96 ± 0.09Ca	1.89 ± 0.06Aa	1.36 ± 0.09Ca	0.21	0.09	0.05	160	1.06 ± 0.02Ca	1.96 ± 0.04Aa	1.38 ± 0.09Ca																																
Water activity	150	0.23 ± 0.00Aa	0.26 ± 0.04Aa	0.18 ± 0.22Aa	0.08	0.12	0.03																																																																																																																																																								
	160	0.21 ± 0.01Aa	0.16 ± 0.03Aa	0.22 ± 0.02Aa				<i>L</i> -Value*	150	64.32 ± 1.19Ca	60.76 ± 0.88Aa	62.80 ± 0.85Ba	0.19	0.14	0.06	160	64.80 ± 1.24Cb	60.41 ± 1.12Aa	63.05 ± 0.67Bb	<i>a</i> -Value*	150	-1.29 ± 0.02Db	-0.44 ± 0.06Aa	-0.51 ± 0.07Ba	0.24	0.1	0.05	160	-1.24 ± 0.01Da	-0.47 ± 0.04Aa	-0.63 ± 0.08Ca	<i>b</i> -Value*	150	4.07 ± 0.12Aa	7.62 ± 0.34Bb	6.67 ± 0.76Db	0.32	0.12	0.08	160	4.17 ± 0.87Aa	8.09 ± 0.83 Bc	8.25 ± 0.43 Dc	TPC	150	13.07 ± 2.13Ba	25.91 ± 1.45Aa	17.14 ± 0.30Aa	0.29	0.16	0.1	160	15.71 ± 0.65Ba	34.75 ± 2.66Aa	25.62 ± 2.21Aa	TTC	150	13.39 ± 2.34Aa	27.59 ± 1.58 a	17.11 ± 0.63Aa	0.25	0.2	0.12	160	18.66 ± 1.41Ab	35.46 ± 2.87 b	26.07 ± 1.50Ab	TFC	150	1.79 ± 0.20Ca	4.84 ± 0.50Aa	2.92 ± 0.23Ca	0.3	0.14	0.09	160	1.98 ± 0.40Ca	5.05 ± 0.06Aa	3.18 ± 0.23Ca	DPPH	150	243.54 ± 4.10Ca	279.93 ± 1.64Aa	233.54 ± 3.09Ca	0.27	0.18	0.08	160	239.72 ± 6.05Ca	305.24 ± 2.59Aa	238.78 ± 1.11Ca	FRAP	150	343.56 ± 3.12Aa	400.52 ± 2.01Aa	413.99 ± 2.33Aa	0.33	0.21	0.11	160	322.29 ± 4.59Aa	522.74 ± 2.47Aa	317.48 ± 8.14Aa	Mitragynine	150	0.96 ± 0.09Ca	1.89 ± 0.06Aa	1.36 ± 0.09Ca	0.21	0.09	0.05	160	1.06 ± 0.02Ca	1.96 ± 0.04Aa	1.38 ± 0.09Ca																																												
<i>L</i> -Value*	150	64.32 ± 1.19Ca	60.76 ± 0.88Aa	62.80 ± 0.85Ba	0.19	0.14	0.06																																																																																																																																																								
	160	64.80 ± 1.24Cb	60.41 ± 1.12Aa	63.05 ± 0.67Bb				<i>a</i> -Value*	150	-1.29 ± 0.02Db	-0.44 ± 0.06Aa	-0.51 ± 0.07Ba	0.24	0.1	0.05	160	-1.24 ± 0.01Da	-0.47 ± 0.04Aa	-0.63 ± 0.08Ca	<i>b</i> -Value*	150	4.07 ± 0.12Aa	7.62 ± 0.34Bb	6.67 ± 0.76Db	0.32	0.12	0.08	160	4.17 ± 0.87Aa	8.09 ± 0.83 Bc	8.25 ± 0.43 Dc	TPC	150	13.07 ± 2.13Ba	25.91 ± 1.45Aa	17.14 ± 0.30Aa	0.29	0.16	0.1	160	15.71 ± 0.65Ba	34.75 ± 2.66Aa	25.62 ± 2.21Aa	TTC	150	13.39 ± 2.34Aa	27.59 ± 1.58 a	17.11 ± 0.63Aa	0.25	0.2	0.12	160	18.66 ± 1.41Ab	35.46 ± 2.87 b	26.07 ± 1.50Ab	TFC	150	1.79 ± 0.20Ca	4.84 ± 0.50Aa	2.92 ± 0.23Ca	0.3	0.14	0.09	160	1.98 ± 0.40Ca	5.05 ± 0.06Aa	3.18 ± 0.23Ca	DPPH	150	243.54 ± 4.10Ca	279.93 ± 1.64Aa	233.54 ± 3.09Ca	0.27	0.18	0.08	160	239.72 ± 6.05Ca	305.24 ± 2.59Aa	238.78 ± 1.11Ca	FRAP	150	343.56 ± 3.12Aa	400.52 ± 2.01Aa	413.99 ± 2.33Aa	0.33	0.21	0.11	160	322.29 ± 4.59Aa	522.74 ± 2.47Aa	317.48 ± 8.14Aa	Mitragynine	150	0.96 ± 0.09Ca	1.89 ± 0.06Aa	1.36 ± 0.09Ca	0.21	0.09	0.05	160	1.06 ± 0.02Ca	1.96 ± 0.04Aa	1.38 ± 0.09Ca																																																								
<i>a</i> -Value*	150	-1.29 ± 0.02Db	-0.44 ± 0.06Aa	-0.51 ± 0.07Ba	0.24	0.1	0.05																																																																																																																																																								
	160	-1.24 ± 0.01Da	-0.47 ± 0.04Aa	-0.63 ± 0.08Ca				<i>b</i> -Value*	150	4.07 ± 0.12Aa	7.62 ± 0.34Bb	6.67 ± 0.76Db	0.32	0.12	0.08	160	4.17 ± 0.87Aa	8.09 ± 0.83 Bc	8.25 ± 0.43 Dc	TPC	150	13.07 ± 2.13Ba	25.91 ± 1.45Aa	17.14 ± 0.30Aa	0.29	0.16	0.1	160	15.71 ± 0.65Ba	34.75 ± 2.66Aa	25.62 ± 2.21Aa	TTC	150	13.39 ± 2.34Aa	27.59 ± 1.58 a	17.11 ± 0.63Aa	0.25	0.2	0.12	160	18.66 ± 1.41Ab	35.46 ± 2.87 b	26.07 ± 1.50Ab	TFC	150	1.79 ± 0.20Ca	4.84 ± 0.50Aa	2.92 ± 0.23Ca	0.3	0.14	0.09	160	1.98 ± 0.40Ca	5.05 ± 0.06Aa	3.18 ± 0.23Ca	DPPH	150	243.54 ± 4.10Ca	279.93 ± 1.64Aa	233.54 ± 3.09Ca	0.27	0.18	0.08	160	239.72 ± 6.05Ca	305.24 ± 2.59Aa	238.78 ± 1.11Ca	FRAP	150	343.56 ± 3.12Aa	400.52 ± 2.01Aa	413.99 ± 2.33Aa	0.33	0.21	0.11	160	322.29 ± 4.59Aa	522.74 ± 2.47Aa	317.48 ± 8.14Aa	Mitragynine	150	0.96 ± 0.09Ca	1.89 ± 0.06Aa	1.36 ± 0.09Ca	0.21	0.09	0.05	160	1.06 ± 0.02Ca	1.96 ± 0.04Aa	1.38 ± 0.09Ca																																																																				
<i>b</i> -Value*	150	4.07 ± 0.12Aa	7.62 ± 0.34Bb	6.67 ± 0.76Db	0.32	0.12	0.08																																																																																																																																																								
	160	4.17 ± 0.87Aa	8.09 ± 0.83 Bc	8.25 ± 0.43 Dc				TPC	150	13.07 ± 2.13Ba	25.91 ± 1.45Aa	17.14 ± 0.30Aa	0.29	0.16	0.1	160	15.71 ± 0.65Ba	34.75 ± 2.66Aa	25.62 ± 2.21Aa	TTC	150	13.39 ± 2.34Aa	27.59 ± 1.58 a	17.11 ± 0.63Aa	0.25	0.2	0.12	160	18.66 ± 1.41Ab	35.46 ± 2.87 b	26.07 ± 1.50Ab	TFC	150	1.79 ± 0.20Ca	4.84 ± 0.50Aa	2.92 ± 0.23Ca	0.3	0.14	0.09	160	1.98 ± 0.40Ca	5.05 ± 0.06Aa	3.18 ± 0.23Ca	DPPH	150	243.54 ± 4.10Ca	279.93 ± 1.64Aa	233.54 ± 3.09Ca	0.27	0.18	0.08	160	239.72 ± 6.05Ca	305.24 ± 2.59Aa	238.78 ± 1.11Ca	FRAP	150	343.56 ± 3.12Aa	400.52 ± 2.01Aa	413.99 ± 2.33Aa	0.33	0.21	0.11	160	322.29 ± 4.59Aa	522.74 ± 2.47Aa	317.48 ± 8.14Aa	Mitragynine	150	0.96 ± 0.09Ca	1.89 ± 0.06Aa	1.36 ± 0.09Ca	0.21	0.09	0.05	160	1.06 ± 0.02Ca	1.96 ± 0.04Aa	1.38 ± 0.09Ca																																																																																
TPC	150	13.07 ± 2.13Ba	25.91 ± 1.45Aa	17.14 ± 0.30Aa	0.29	0.16	0.1																																																																																																																																																								
	160	15.71 ± 0.65Ba	34.75 ± 2.66Aa	25.62 ± 2.21Aa				TTC	150	13.39 ± 2.34Aa	27.59 ± 1.58 a	17.11 ± 0.63Aa	0.25	0.2	0.12	160	18.66 ± 1.41Ab	35.46 ± 2.87 b	26.07 ± 1.50Ab	TFC	150	1.79 ± 0.20Ca	4.84 ± 0.50Aa	2.92 ± 0.23Ca	0.3	0.14	0.09	160	1.98 ± 0.40Ca	5.05 ± 0.06Aa	3.18 ± 0.23Ca	DPPH	150	243.54 ± 4.10Ca	279.93 ± 1.64Aa	233.54 ± 3.09Ca	0.27	0.18	0.08	160	239.72 ± 6.05Ca	305.24 ± 2.59Aa	238.78 ± 1.11Ca	FRAP	150	343.56 ± 3.12Aa	400.52 ± 2.01Aa	413.99 ± 2.33Aa	0.33	0.21	0.11	160	322.29 ± 4.59Aa	522.74 ± 2.47Aa	317.48 ± 8.14Aa	Mitragynine	150	0.96 ± 0.09Ca	1.89 ± 0.06Aa	1.36 ± 0.09Ca	0.21	0.09	0.05	160	1.06 ± 0.02Ca	1.96 ± 0.04Aa	1.38 ± 0.09Ca																																																																																												
TTC	150	13.39 ± 2.34Aa	27.59 ± 1.58 a	17.11 ± 0.63Aa	0.25	0.2	0.12																																																																																																																																																								
	160	18.66 ± 1.41Ab	35.46 ± 2.87 b	26.07 ± 1.50Ab				TFC	150	1.79 ± 0.20Ca	4.84 ± 0.50Aa	2.92 ± 0.23Ca	0.3	0.14	0.09	160	1.98 ± 0.40Ca	5.05 ± 0.06Aa	3.18 ± 0.23Ca	DPPH	150	243.54 ± 4.10Ca	279.93 ± 1.64Aa	233.54 ± 3.09Ca	0.27	0.18	0.08	160	239.72 ± 6.05Ca	305.24 ± 2.59Aa	238.78 ± 1.11Ca	FRAP	150	343.56 ± 3.12Aa	400.52 ± 2.01Aa	413.99 ± 2.33Aa	0.33	0.21	0.11	160	322.29 ± 4.59Aa	522.74 ± 2.47Aa	317.48 ± 8.14Aa	Mitragynine	150	0.96 ± 0.09Ca	1.89 ± 0.06Aa	1.36 ± 0.09Ca	0.21	0.09	0.05	160	1.06 ± 0.02Ca	1.96 ± 0.04Aa	1.38 ± 0.09Ca																																																																																																								
TFC	150	1.79 ± 0.20Ca	4.84 ± 0.50Aa	2.92 ± 0.23Ca	0.3	0.14	0.09																																																																																																																																																								
	160	1.98 ± 0.40Ca	5.05 ± 0.06Aa	3.18 ± 0.23Ca				DPPH	150	243.54 ± 4.10Ca	279.93 ± 1.64Aa	233.54 ± 3.09Ca	0.27	0.18	0.08	160	239.72 ± 6.05Ca	305.24 ± 2.59Aa	238.78 ± 1.11Ca	FRAP	150	343.56 ± 3.12Aa	400.52 ± 2.01Aa	413.99 ± 2.33Aa	0.33	0.21	0.11	160	322.29 ± 4.59Aa	522.74 ± 2.47Aa	317.48 ± 8.14Aa	Mitragynine	150	0.96 ± 0.09Ca	1.89 ± 0.06Aa	1.36 ± 0.09Ca	0.21	0.09	0.05	160	1.06 ± 0.02Ca	1.96 ± 0.04Aa	1.38 ± 0.09Ca																																																																																																																				
DPPH	150	243.54 ± 4.10Ca	279.93 ± 1.64Aa	233.54 ± 3.09Ca	0.27	0.18	0.08																																																																																																																																																								
	160	239.72 ± 6.05Ca	305.24 ± 2.59Aa	238.78 ± 1.11Ca				FRAP	150	343.56 ± 3.12Aa	400.52 ± 2.01Aa	413.99 ± 2.33Aa	0.33	0.21	0.11	160	322.29 ± 4.59Aa	522.74 ± 2.47Aa	317.48 ± 8.14Aa	Mitragynine	150	0.96 ± 0.09Ca	1.89 ± 0.06Aa	1.36 ± 0.09Ca	0.21	0.09	0.05	160	1.06 ± 0.02Ca	1.96 ± 0.04Aa	1.38 ± 0.09Ca																																																																																																																																
FRAP	150	343.56 ± 3.12Aa	400.52 ± 2.01Aa	413.99 ± 2.33Aa	0.33	0.21	0.11																																																																																																																																																								
	160	322.29 ± 4.59Aa	522.74 ± 2.47Aa	317.48 ± 8.14Aa				Mitragynine	150	0.96 ± 0.09Ca	1.89 ± 0.06Aa	1.36 ± 0.09Ca	0.21	0.09	0.05	160	1.06 ± 0.02Ca	1.96 ± 0.04Aa	1.38 ± 0.09Ca																																																																																																																																												
Mitragynine	150	0.96 ± 0.09Ca	1.89 ± 0.06Aa	1.36 ± 0.09Ca	0.21	0.09	0.05																																																																																																																																																								
	160	1.06 ± 0.02Ca	1.96 ± 0.04Aa	1.38 ± 0.09Ca																																																																																																																																																											

^a Values are presented as mean ± SD ($n = 3$). Different uppercase letters within the same row indicate significant differences ($p \leq 0.05$) among wall materials. Different lowercase letters within the same column indicate significant differences ($p \leq 0.05$) between temperatures. Means sharing the same letter are not significantly different according to Tukey's HSD test.

temperature ($\eta^2 = 0.10$). Higher temperatures improved solubility slightly, likely through reduced moisture and better particle formation (Table 2), with the highest solubility observed in microcapsules coated with resistant maltodextrin (95.8 ± 0.09%). The branched structure of resistant maltodextrin enhances its density, and the presence of hydroxyl groups allows it to bond with water molecules effectively, resulting in superior solubility compared to those coated with gum arabic or a combination of both.⁵¹ In addition, higher temperatures reduce residual moisture, enhancing particle dispersibility; low moisture (MC) minimizes clumping upon reconstitution.

The large, porous amorphous structure of the microcapsules using resistant maltodextrin as the coating material facilitates easy dissolution in water, aligning with the findings of Jordán *et al.* (2018),⁵² which indicated that resistant maltodextrin-coated microcapsules have better solubility than those coated with gum arabic. Additionally, increasing the inlet drying temperature from 150 °C to 160 °C improved the water solubility of microcapsules coated with gum arabic and the combination of gum arabic and resistant maltodextrin. The higher drying temperature reduces moisture content, thereby enhancing the ability of the microcapsules to dissolve in water. In other words, tackiness affects internal evaporation but not

external solubility; lower moisture content from optimal temperatures aids dissolution. This is consistent with the research of Astina and Sapwarobol (2019),⁵¹ which showed that lower moisture content improves the solubility of powdered milk.

3.5 Color parameters (L^* , a^* , b^*) of KLE microcapsules

Color attributes (L^* , a^* , b^*) showed meaningful changes as indicated in Table 2. Lightness (L^* ; 60.4–64.8) was moderately influenced by both the carrier ($\eta^2 = 0.19$) and temperature ($\eta^2 = 0.14$). The a^* values (-1.29 to -0.44) showed a strong wall material effect ($\eta^2 = 0.24$), reflecting GA's tendency toward less negative redness–greenness. The b^* values (4.1–8.3) showed the strongest carrier effect ($\eta^2 = 0.32$), confirming the distinct visual profiles imparted by GA.

The L^* value, which ranges from 0 (dark) to 100 (light), showed that microcapsules coated with resistant maltodextrin were lighter than those coated with gum arabic or a combination of both. This is because resistant maltodextrin is a white powder, resulting in a bright white color when dissolved in water, whereas gum arabic is a light-yellow powder that turns brown when dissolved. Therefore, microcapsules with resistant maltodextrin as the coating material appeared lighter than



those with gum arabic. The inlet drying temperature did not significantly affect the L^* value of the microcapsules ($p \leq 0.05$).

The a^* value indicates the red–green spectrum, with negative values representing green and positive values representing red. Similarly, the b^* value indicates the yellow–blue spectrum, with positive values representing yellow. An increase in the inlet drying temperature from 150 °C to 160 °C resulted in higher b^* values for KLE microcapsules. This is attributed to the Maillard reaction, which intensifies yellow coloration at higher temperatures.⁵³

3.6 Phytochemical properties of KLE microcapsules

3.6.1 Total phenolic content. From Table 2, it was observed that total phenolic content (TPC) ranged from 13.1 to 34.8 mg GAE per mL and was strongly influenced by the wall material ($\eta^2 = 0.29$), with GA promoting higher retention. Temperature contributed moderately ($\eta^2 = 0.16$), suggesting heat-stimulated release or degradation depending on the carrier type. When considering the impact of temperature, increasing the inlet temperature from 150 °C to 160 °C resulted in a higher total phenolic content in the microcapsules. The higher temperature facilitated faster drying and the formation of a protective film layer around the microcapsules, which shortens the exposure time of the phenolic compounds to heat. Additionally, higher drying temperatures may possibly induce faster film formation and polymerization reactions that could lead to an increase in the total phenolic content.⁵⁴

Regarding the coating material, microcapsules coated with gum arabic demonstrated a higher total phenolic content compared to those coated with resistant maltodextrin or a combination of resistant maltodextrin and gum arabic. This is because gum arabic has emulsifying properties that enhance stability and can form a well-structured polymer film around the microcapsules.⁵⁵

3.6.2 Total flavonoid content. The results shown in Table 2 revealed that total flavonoid content (TFC) varied between 1.8 and 5.1 mg QE per g. The carrier effect was again dominant ($\eta^2 = 0.30$), with GA-based formulations consistently demonstrating higher content. Specifically, microcapsules coated with gum arabic exhibited the highest total flavonoid content. This is due to the matrix formation between the gum arabic coating and the core substance, which helps reduce the loss of total flavonoid content. Additionally, the emulsifying properties of gum arabic enhance stability and protect the active compounds from environmental conditions.⁵⁶

In contrast, the inlet temperature during spray drying (150 °C and 160 °C) did not significantly affect the total flavonoid content. Increasing the inlet temperature from 150 °C to 160 °C did not significantly impact the total flavonoid content ($p > 0.05$). Flavonoids may be more heat-stable or better protected by the matrix; TPC includes broader reducing species sensitive to heat. The microcapsules coated with gum arabic had the highest total flavonoid content at both 150 °C and 160 °C (4.98 ± 0.8 and 5.22 ± 0.12 mg QE per g db., respectively), followed by those coated with resistant maltodextrin combined with gum arabic (3.08 ± 0.23 and 2.99 ± 0.35 mg QE per g db., respectively), and finally those coated

solely with resistant maltodextrin (1.67 ± 0.5 and 1.61 ± 0.72 mg QE per g db., respectively).

3.6.3 Antioxidant activity using the DPPH assay. The results revealed that antioxidant activity showed strong wall material effects. DPPH scavenging activity ranged from 233.5 to 305.2 $\mu\text{mol TE per } 100 \text{ g}$ ($\eta^2 = 0.27$), as can be seen in Table 2. Gum arabic preserved and even enhanced antioxidant activity compared to resistant maltodextrin.

Increasing the inlet temperature during spray drying resulted in a corresponding increase in the antioxidant activity, which can be explained by the higher drying temperature enhancing the antioxidant properties of the microcapsules.⁴⁷ This trend is attributed to the direct correlation between antioxidant activity and phenolic compound content; higher levels of phenolic compounds generally lead to increased antioxidant activity.⁵⁷

3.6.4 Antioxidant activity using the FRAP assay. As can be observed from Table 2, the results indicated that the FRAP varied more broadly (317.5–522.7 $\mu\text{mol TE per } 100 \text{ g}$), with both the carrier ($\eta^2 = 0.33$) and temperature ($\eta^2 = 0.21$) being important. Gum arabic preserved and even enhanced antioxidant activity compared to resistant maltodextrin.

When examining the type of the coating material, microcapsules coated with gum arabic and those coated with a combination of resistant maltodextrin and gum arabic showed no statistically significant difference in FRAP antioxidant activity. However, gum arabic-coated microcapsules demonstrated higher antioxidant activity compared to those coated with resistant maltodextrin. This is because the film layer formed by gum arabic better prevents oxidation reactions compared to resistant maltodextrin.⁵⁸

Regarding the temperature factor, increasing the inlet temperature in the spray drying process from 150 °C to 160 °C resulted in a significant change in FRAP antioxidant activity ($p \leq 0.05$). This could be attributed to the higher inlet temperature causing microcapsule particles to crack, which leads to direct exposure of antioxidants to heat and subsequent loss due to direct heat exposure.⁵⁹

3.6.5 Total tannin content. The results presented in Table 2 revealed that total tannin content (TTC) followed a similar trend (13.4–35.5 mg CE per g), with both the carrier ($\eta^2 = 0.25$) and temperature ($\eta^2 = 0.20$) exerting effects, highlighting synergistic contributions. It was found that both the type of coating material and the inlet temperature during spray drying at 150 °C and 160 °C significantly affect the total tannin content. Specifically, microcapsules coated with gum arabic and processed at an inlet temperature of 160 °C exhibited the highest total tannin content (36.42 ± 2.45 mg TAE per g).

Increasing the inlet temperature from 150 °C to 160 °C resulted in a higher total tannin content in the microcapsules. This is because the higher temperature facilitates the formation of a well-structured film layer on the particle walls, which enhances the retention of tannins. Regarding the coating material, microcapsules using gum arabic as the coating material demonstrated a higher total tannin content compared to those coated with resistant maltodextrin or a combination of resistant maltodextrin and gum arabic. This is due to gum



arabic's emulsifying properties, which improve stability and enable the formation of a polymer film around the microcapsules, similar to its effect on total phenolic content.⁵⁵

3.6.6 Mitragynine stability. The chromatographic profile of kratom leaf extract (KLE), as revealed by HPLC analysis, demonstrated a distinct and well-resolved peak at approximately 6.9 min, corresponding to mitragynine (Fig. 2). This identification was confirmed through comparison with an authentic standard, consistent with previous reports that place mitragynine's retention time between 6.5 and 7.0 min under reversed-phase conditions.^{60,61} The sharp symmetry and high intensity of this peak affirm mitragynine's predominance among the alkaloids present in kratom leaf extract (KLE). Additional minor peaks observed between 2–5 min and 7–10 min likely represent polar phenolic compounds and structurally related alkaloids such as paynantheine and speciogynine.

The developed HPLC method exhibited a stable baseline and absence of interfering signals beyond 10 min, indicating high selectivity and robustness. These attributes are essential for reliable quantification of mitragynine in complex plant matrices and support the method's suitability for routine analysis in quality control and formulation studies.

Encapsulation studies further revealed that the retention of mitragynine in spray-dried microcapsules was significantly influenced by the choice of the wall material. Gum arabic (GA) consistently yielded the highest mitragynine content (1.89–1.96 mg per g), outperforming resistant maltodextrin (RMD) and the RMD–GA blend. This superior performance is

attributed to GA's highly branched polysaccharide structure and emulsifying properties, which enhance molecular entrapment and protect bioactives from thermal and oxidative degradation during spray drying.^{62,63} In contrast, RMD, while beneficial for moisture reduction and solubility, demonstrated lower encapsulation efficiency for hydrophobic alkaloids like mitragynine, likely due to its limited molecular affinity.⁶⁴

Interestingly, inlet temperature (150 vs. 160 °C) did not significantly affect mitragynine retention across formulations, suggesting that wall material composition exerts a more dominant influence than thermal stress. This observation aligns with previous findings that emphasize the role of carrier-core interactions over processing temperature in determining encapsulation outcomes (Díaz-Montes, 2023).⁶³

Moreover, the retention trends of mitragynine paralleled those of total phenolic content (TPC) and antioxidant activity (DPPH and FRAP), reinforcing the protective role of GA in preserving multiple classes of bioactives. The co-stabilization of alkaloids and phenolics is particularly relevant for the development of functional food and nutraceutical products, where both pharmacological efficacy and antioxidant potential are desired.⁶²

Collectively, these findings underscore the importance of wall material selection in microencapsulation strategies for botanical extracts. Gum arabic, particularly at an inlet temperature of 160 °C, offers a promising formulation for preserving mitragynine and related bioactives, thereby enhancing the stability and functionality of KLE-based products.

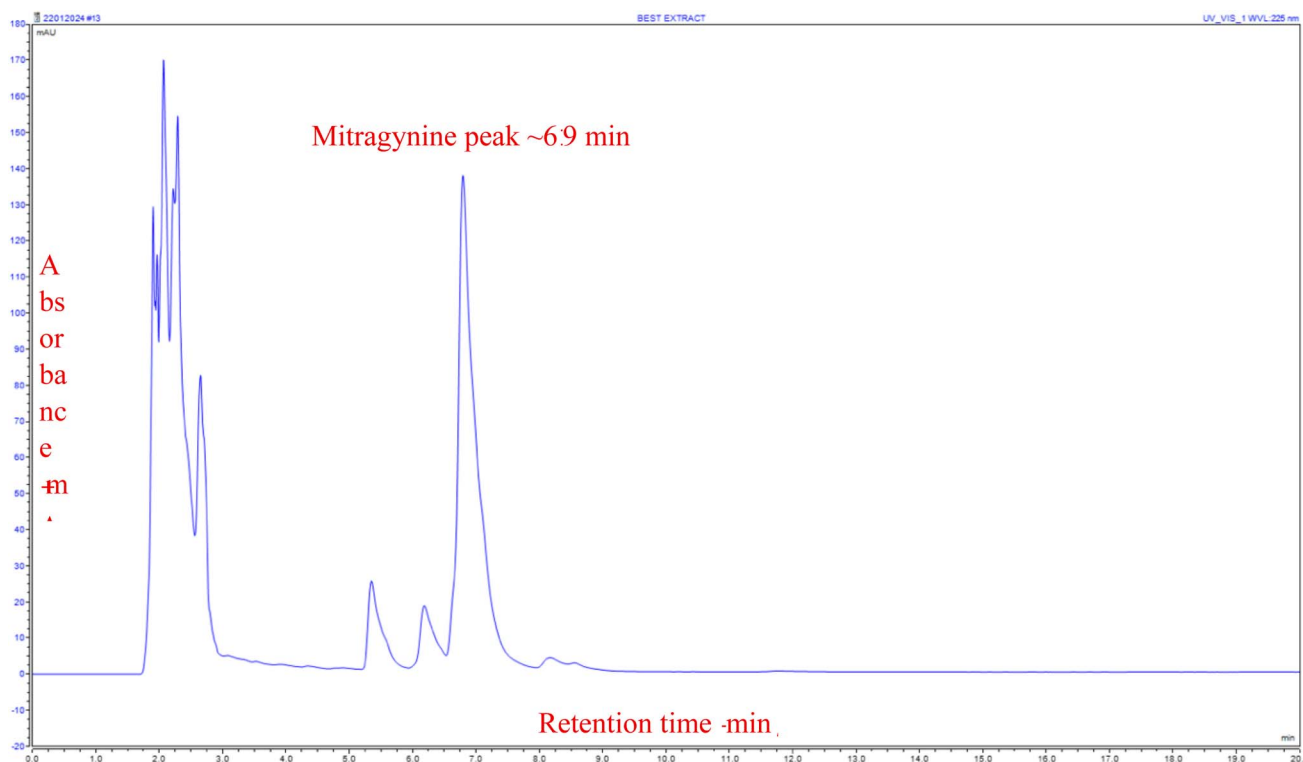


Fig. 2 HPLC chromatogram of kratom leaf extract (KLE), showing the major alkaloid mitragynine at a retention time of approximately 6.9 min and minor peaks corresponding to other alkaloids and phenolic compounds. X-Axis: retention time (min); Y-axis: absorbance (mAU).



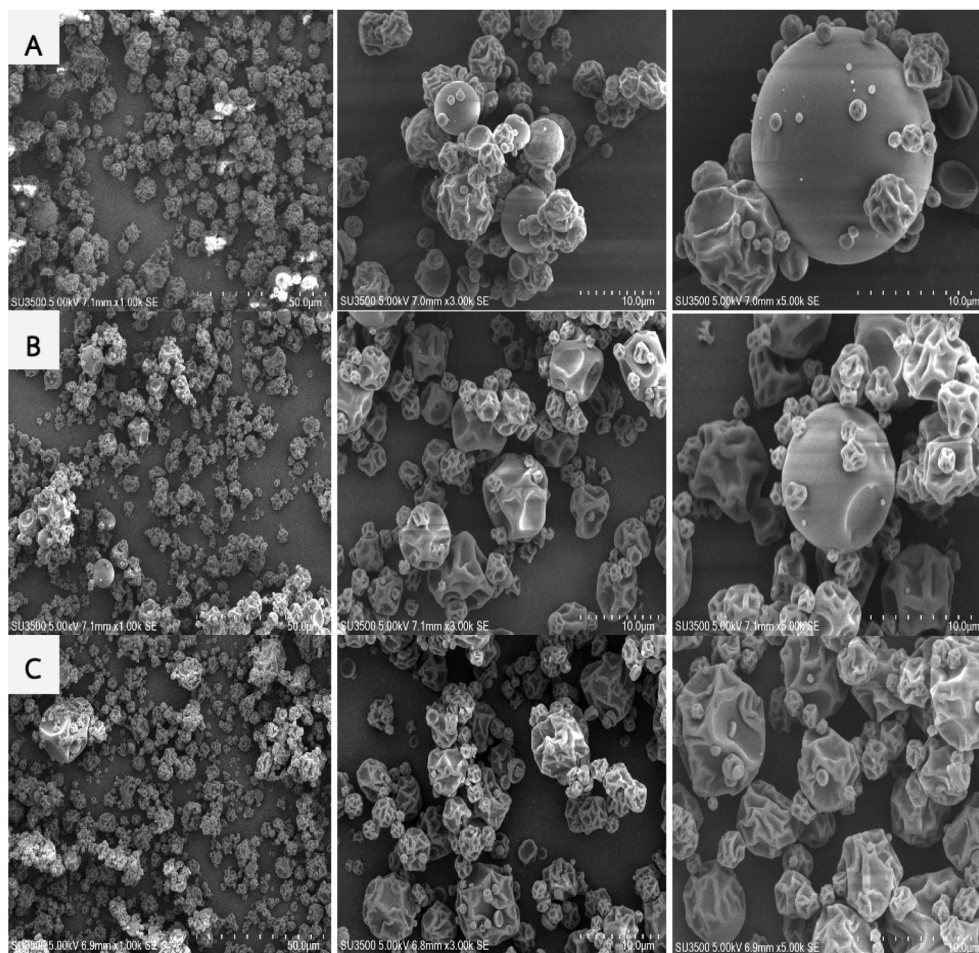


Fig. 3 Scanning electron microscopy images at magnifications of 1000 \times , 3000 \times , and 5000 \times (left to right) of KLE microcapsules obtained at an inlet temperature of 150 $^{\circ}$ C: (A) coated with resistant maltodextrin DE10, (B) coated with gum arabic, and (C) coated with a 1 : 1 ratio of resistant maltodextrin and gum arabic.

3.7 Surface structure of KLE microcapsules analyzed by scanning electron microscopy (SEM)

The shape and structure of KLE microcapsules are influenced by various production factors, including the type of the coating material, coating concentration, coating-to-liquid ratio, solution viscosity, inlet temperature of the spray dryer, and the flow rate of the solution through the spray dryer. These factors not only affect the visual appearance of the microcapsules but also impact the stability of the bioactive compounds within them. A smoother morphology in GA-coated microcapsules is associated with higher bioactive retention due to reduced surface exposure. Structural defects such as cracks or surface ruptures can decrease encapsulation efficiency and facilitate moisture infiltration, potentially leading to oxidation of the active compounds.^{65,66}

Fig. 3a illustrates the morphology of microcapsules coated with resistant maltodextrin at an inlet temperature of 150 $^{\circ}$ C. Analyzed using scanning electron microscopy (SEM) at magnifications of 1000 \times , 3000 \times , and 5000 \times , these microcapsules generally appear spherical with relatively smooth surfaces and minor folds and dents, indicating effective encapsulation. Some particles tend to cluster slightly, which may be due to residual

moisture in the coating material or moisture absorbed from the environment.⁶⁷

The morphology of microcapsules coated with gum arabic at 150 $^{\circ}$ C is shown in Fig. 3b. These particles are typically smaller and exhibit more surface folds and dents compared to those coated with resistant maltodextrin. The increased surface irregularities are attributed to the rapid formation of the coating during the initial stage, leading to the swift evaporation of water within the particles.⁶⁸

Fig. 3c also depicts microcapsules coated with a 1 : 1 ratio of resistant maltodextrin and gum arabic at 150 $^{\circ}$ C. These microcapsules are mostly spherical with a mix of large and small particles. They show a tendency to be well-distributed without significant clustering but exhibit more surface folds and dents compared to capsules coated solely with resistant maltodextrin. This morphology is influenced by factors such as direct exposure to heat and rapid evaporation of water within the particles, leading to deformation and surface folding.⁶⁷

At a higher inlet temperature of 160 $^{\circ}$ C, Fig. 4a shows microcapsules coated with resistant maltodextrin. The particles are mostly spherical with larger sizes and some smaller particles clumped together. The surface exhibits wrinkles and is partially



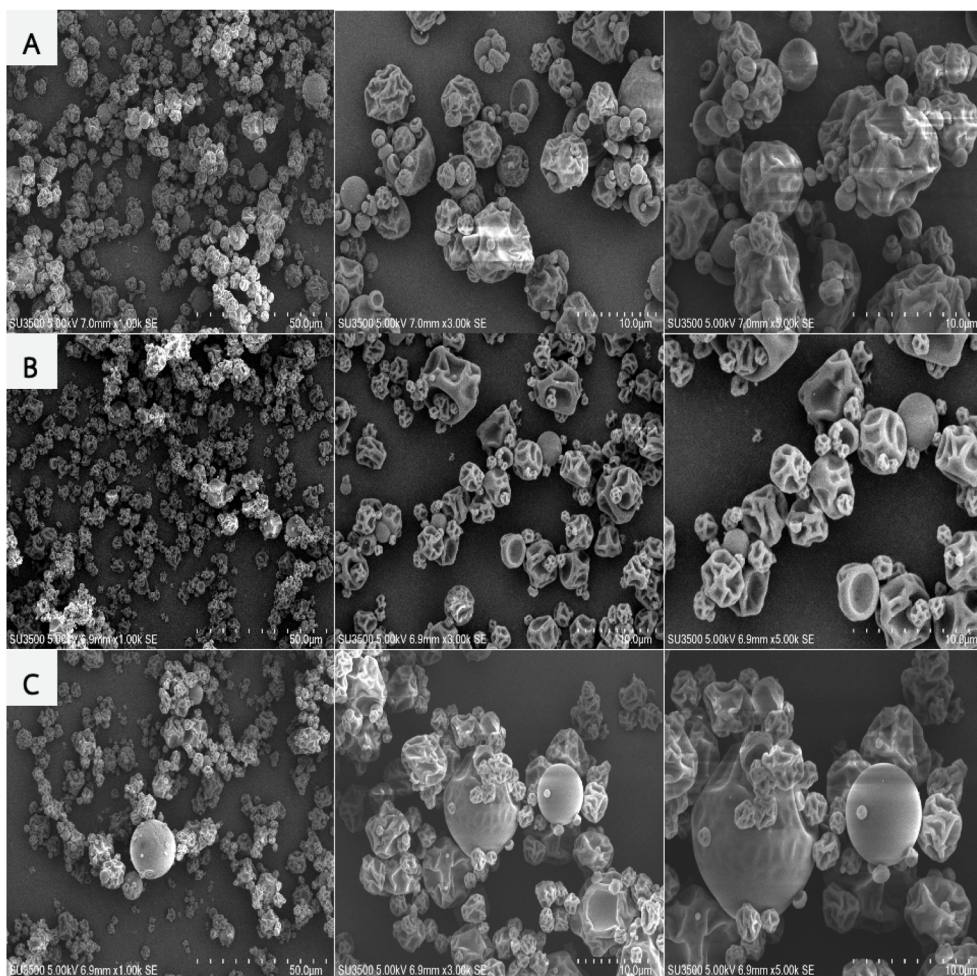


Fig. 4 Scanning electron microscopy images at magnifications of 1000 \times , 3000 \times , and 5000 \times (left to right) of KLE microcapsules obtained at an inlet temperature of 160 $^{\circ}$ C: (A) coated with resistant maltodextrin DE10, (B) coated with gum arabic, and (C) coated with a 1 : 1 ratio of resistant maltodextrin and gum arabic.

smooth. In contrast, Fig. 4b presents microcapsules coated with gum arabic, which are generally smaller with a rough surface and significant wrinkling and crumpling. Fig. 4c depicts microcapsules coated with a 1 : 1 ratio of resistant maltodextrin and gum arabic. These particles are small with a rough surface, showing pronounced crumpling and indentations compared to single coatings.

These observations highlight how different coating materials and inlet temperatures affect the structural characteristics of microcapsules. Higher temperatures and certain coating combinations can result in increased surface roughness and crumpling, which impacts the integrity and performance of the microcapsules.⁶⁹

3.8. Quality changes of KLE microcapsules during storage

3.8.1 Changes in the physical properties of KLE microcapsules during storage. Fig. 5a and b show the moisture content and water activity of the KLE microcapsules, respectively. The initial moisture content of the KLE microcapsules was $2.65 \pm 0.1\%$. Over time, the moisture content increased to

$2.75 \pm 0.2\%$, $2.85 \pm 0.25\%$, $2.94 \pm 0.15\%$, $3.05 \pm 0.2\%$, $3.22 \pm 0.1\%$, and $3.33 \pm 0.16\%$ after 15, 30, 45, 60, 75, and 90 days of storage, respectively. The initial water activity of the KLE microcapsules was 0.164 ± 0.03 . With prolonged storage, the water activity increased to 0.193 ± 0.07 , 0.221 ± 0.04 , 0.243 ± 0.01 , 0.256 ± 0.04 , 0.289 ± 0.07 , and 0.317 ± 0.03 after 15, 30, 45, 60, 75, and 90 days, respectively.

The moisture content and free water of the KLE microcapsules did not exceed the spoilage indicator set (moisture content $\leq 5\%$ and water activity < 0.6) even after 90 days of storage. This is due to the aluminum foil packaging's excellent ability to prevent moisture and water vapor from the environment.⁷⁰ Aluminum foil has a water vapor transmission rate of $0.06571 \text{ g per m}^2 \text{ per day}$ and an oxygen transmission rate of $0.00873 \text{ mL per m}^2 \text{ per day}$, respectively.⁷¹ This low permeability explains why the aluminum foil packaging minimizes water and oxygen absorption under vacuum, resulting in only a slight increase in moisture and free water content. Water activity can serve as an indicator of product stability against oxidation reactions, such as fat oxidation and rancidity. A water activity of



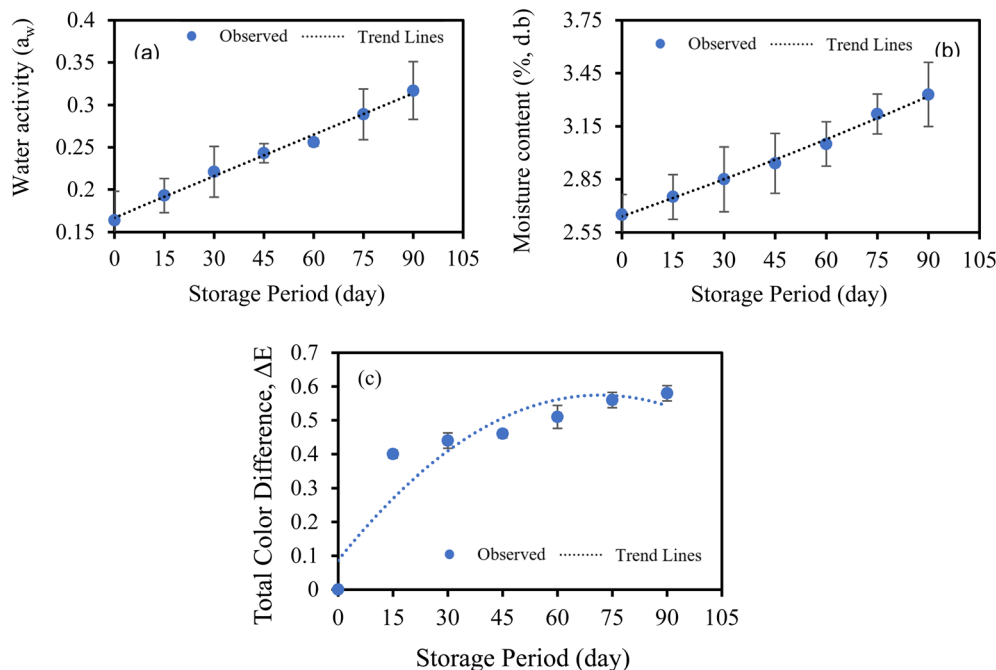


Fig. 5 Moisture content (a), water activity (b), and total color difference (c) of stored KLE microcapsules at different storage periods. Values represent means \pm SD ($n = 3$).

less than 0.6 indicates that the sample remains stable or has good shelf stability.⁷² These results are consistent with those of ref. 73 which studied the storage of papaya powder in aluminum foil bags and found that the water activity of the papaya powder remained below 0.6 after 7 weeks of storage.

The progressive increase in total color difference (ΔE) observed in spray-dried KLE microcapsules over the 90-day storage period reflects gradual pigment degradation and structural changes within the microcapsules. Initially, the ΔE value was 0 on day 0, indicating no perceptible color change. A marked increase to $\Delta E = 0.40$ by day 15 suggests an early phase of rapid color modification. This may be attributed to residual moisture and initial oxidative reactions, which are known to affect polyphenolic compounds and sensitive pigments.⁷⁴

Following this initial phase, the rate of color change decelerated, with ΔE values reaching 0.44 and 0.46 on days 30 and 45, respectively. This plateau-like behavior implies that the encapsulated system may have achieved a degree of equilibrium in pigment stability and wall matrix integrity, thereby reducing the rate of further degradation. Similar stabilization trends have been reported in encapsulated anthocyanins and carotenoids, where wall materials such as maltodextrin and gum arabic mitigate oxidative stress and thermal instability.⁷⁵

Between days 60 and 90, ΔE values continued to increase gradually from 0.51 to 0.58, indicating ongoing but limited degradation. This phase likely involves slower oxidative processes and potential Maillard-type reactions, which are common during prolonged storage of encapsulated bioactives.⁷⁶ Importantly, the final ΔE value remained below 1.0, a threshold generally considered imperceptible or only slightly noticeable to the human eye. This suggests that the encapsulation matrix

provided effective protection against color deterioration, preserving the visual quality of the product.

Overall, these findings demonstrate that the selected encapsulation strategy offers substantial color stability over time. The minor perceptible changes observed after three months of storage underscore the efficacy of the wall materials in limiting oxidative and thermal degradation of sensitive compounds. This stability is critical for maintaining both the aesthetic and functional attributes of KLE microcapsules, particularly in applications where visual appeal and bioactive retention are essential.

3.8.2 Changes in total phenolic content during storage.

Fig. 6a shows the decrease in total phenolic content in KLE microcapsules during storage. Initially, the total phenolic content of the microcapsules was 36.78 ± 3.08 mg GAE per g. Over time, this amount gradually decreased, with total phenolic content measuring 34.83 ± 1.52 , 33.20 ± 0.65 , 32.66 ± 1.04 , 31.88 ± 0.67 , 30.36 ± 0.89 , and 30.10 ± 0.45 mg GAE per g at 15, 30, 45, 60, 75, and 90 days of storage, respectively. Several factors can lead to the reduction in total phenolic content, including temperature, increased moisture, and the amount of air permeating the packaging and coming into contact with the product.⁷⁷ These results align with those of ref. 78, which found a reduction in phenolic content in ground coffee stored in aluminum foil bags.

3.8.3 Changes in total flavonoid content during storage.

Fig. 6b displays the decrease in total flavonoid content in KLE microcapsules during storage. The initial total flavonoid content was 5.22 ± 0.12 mg QE per g. This amount gradually decreased over time, with values of 5.15 ± 0.15 , 4.95 ± 0.09 , 4.85 ± 0.23 , 4.75 ± 0.12 , 4.54 ± 0.15 , and 4.32 ± 0.05 mg QE per g at



15, 30, 45, 60, 75, and 90 days of storage, respectively. Key factors affecting the total flavonoid content include temperature, light, and oxygen. The primary cause of the decrease in flavonoid content is oxidation during storage, a common reaction in food preservation. This hypothesis aligns with that of ref. 79, which studied the stability of bioactive compounds in rowan berries. Their study found that flavonoid levels in berries decreased by up to 86% during 20 weeks of storage. Therefore, oxidation directly impacts the reduction in flavonoid content. Similarly, a previous study⁸⁰ examined the impact of packaging material on the quality of powdered milk over 12 months. They found that powdered milk packaged in aluminum foil experienced a lower reduction in flavonoids compared to other packaging materials, as aluminum foil blocks light and has low moisture and oxygen permeability. This indicates that the packaging material directly affects the reduction in total flavonoid content in KLE microcapsules.

3.8.4 Changes in total tannin content during storage.

Fig. 6c illustrates the decrease in total tannin content in KLE microcapsules during storage. The initial total tannin content was 36.42 ± 2.45 mg TAE per g. Over time, this amount gradually decreased, with total tannin content measuring 33.83 ± 1.25 , 32.20 ± 1.56 , 31.66 ± 1.05 , 30.75 ± 0.85 , 29.29 ± 0.45 , and 29.08 ± 0.06 mg TAE per g at 15, 30, 45, 60, 75, and 90 days of storage, respectively. This trend mirrors the decrease observed in total phenolic content and total flavonoid content, which also decreased with extended storage time. These findings are consistent with those of ref. 81, which investigated tannin extraction from kluwek fruits and its stability. Their study found that tannin extracted from kluwek fruits and stored in opaque glass containers had a shelf life of about 15 days, while tannins

exposed to air and light had a shelf life of only 9 h. The darker color of kluwek fruit extracts may result from direct light exposure, which increases light absorption and accelerates oxidation reactions that can degrade tannins.⁸² Thus, packaging, light, and temperature are crucial factors affecting the stability and shelf life of KLE microcapsules.

3.8.5 Changes in antioxidant activity (DPPH) and antioxidant activity (FRAP) during storage.

Fig. 7a illustrates the reduction in antioxidant activity of KLE microcapsules as measured by the DPPH method during storage. Initially, the antioxidant activity was 293.55 ± 3.28 μ M TE per 100 g. This value gradually decreased over time, reaching 283.06 ± 5.76 , 271.45 ± 4.32 , 265.53 ± 2.15 , 258.06 ± 3.52 , 247.65 ± 2.85 , and 227.88 ± 4.64 μ M TE per 100 g at 15, 30, 45, 60, 75, and 90 days, respectively. This trend is consistent with the decrease in total phenolic content, as phenolics are directly related to antioxidant activity.⁸³ A study by ref. 80 on the antioxidant activity of commercial powdered milk using the DPPH method found a 42.37% reduction in antioxidant activity over one year of storage. Their results indicated that the packaging material significantly affects the antioxidant activity.

Similarly, antioxidant activity measured by the FRAP method also showed a decline trend over time (Fig. 7b). The FRAP values for the KLE microcapsules were 522.74 ± 2.47 , 477.49 ± 3.56 , 469.32 ± 3.12 , 459.35 ± 2.76 , 435.56 ± 5.62 , 422.63 ± 2.89 , and 409.67 ± 8.51 μ M TE per 100 g at days 1, 15, 30, 45, 60, 75, and 90, respectively. The observed reduction in antioxidant activity during storage indicates that antioxidant capacity decreases with prolonged storage time, and the packaging material plays a crucial role in preserving the antioxidant activity of KLE microcapsules.

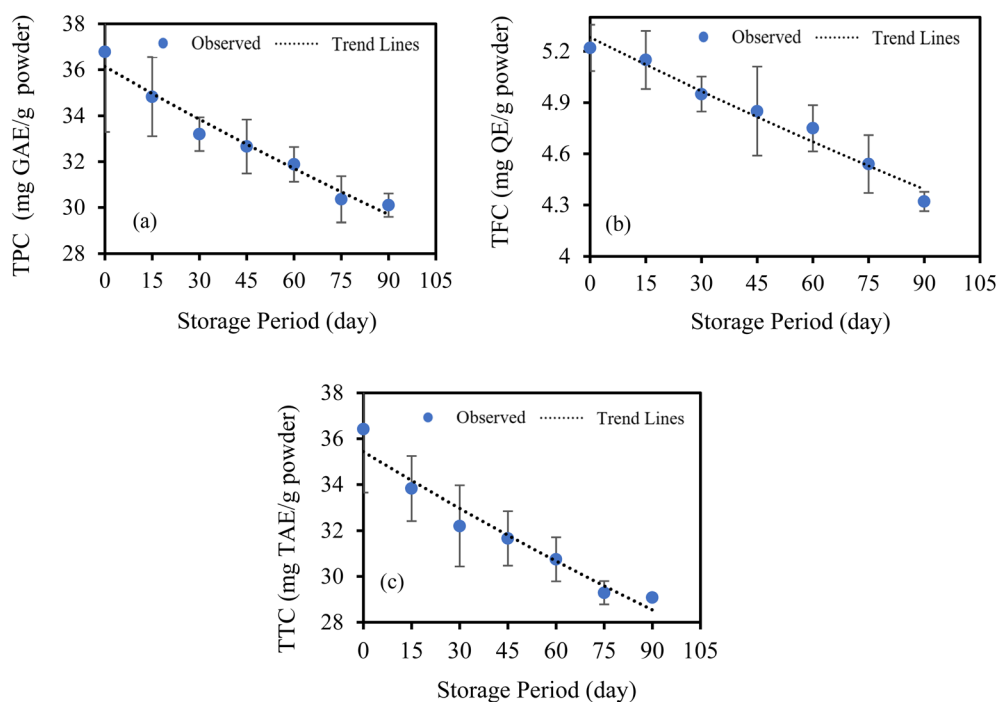


Fig. 6 Total phenolic content (TPC, a), total flavonoid content (TFC, b), and total tannin content (TTC, c) of stored KLE microcapsules at different storage periods. Values represent means \pm SD ($n = 3$).



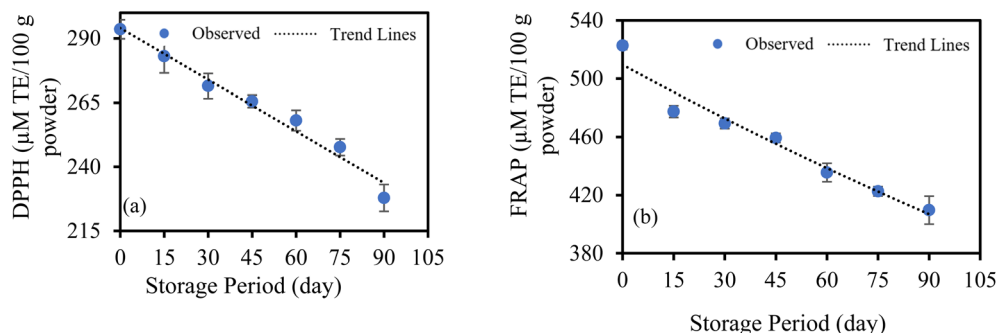


Fig. 7 Antioxidant activities of stored KLE microcapsules measured by (a) DPPH radical-scavenging assay and (b) FRAP assay. Values represent means \pm SD ($n = 3$). DPPH = 2,2-diphenyl-1-picrylhydrazyl; FRAP = ferric-reducing antioxidant power.

Table 3 Statistical parameters of the models used in the study and the predicted shelf life of KLE microcapsules using GA at 160 °C

Properties	Parameter	Zero-order model		First-order model		Predicted shelf life (day)
		Values	CI (95%)	Values	CI (95%)	
Moisture content (%)	C_0	2.629	(2.58, 2.68)	2.639	(2.61, 2.67)	92.55
	k	-0.008	(-0.008, -0.007)	-0.003	(-0.003, -0.002)	
	R^2	0.991		0.995		
Water activity	C_0	0.167	(0.158, 0.176)	0.174	(0.163, 0.185)	91.88
	k	-0.002	(-0.002, -0.001)	-0.007	(-0.008, -0.006)	
	R^2	0.992		0.986		
TPC (mg GAE per g db.)	C_0	36.076	(35.14, 37.02)	36.193	(35.32, 37.07)	82.84
	k	0.072	(0.055, 0.089)	0.002	(0.002, 0.003)	
	R^2	0.958		0.966		
TTC (mg TAE per g db.)	C_0	35.378	(34.13, 36.63)	35.528	(34.35, 36.7)	81.26
	k	0.078	(0.054, 0.10)	0.002	(0.002, 0.003)	
	R^2	0.937		0.949		
TFC (mg QE per g db.)	C_0	5.267	(5.18, 5.36)	5.275	(5.17, 5.38)	96.55
	k	0.010	(0.008, 0.011)	0.002	(0.0016, 0.0024)	
	R^2	0.978		0.972		
DPPH (μ M TE per 100 g db.)	C_0	294.014	(287.14, 300.89)	294.743	(286.74, 302.75)	98.77
	k	0.670	(0.54, 0.80)	0.003	(0.002, 0.003)	
	R^2	0.973		0.967		
FRAP (μ M TE per 100 g db.)	C_0	508.397	(491.3, 525.17)	510.410	(494.2, 526.6)	85.90
	k	1.149	(0.84, 1.46)	0.003	(0.0019, 0.0032)	
	R^2	0.948		0.955		
Integrated shelf-life decision (minimum across attributes)	—	—	—	—	—	81.26

3.9. Kinetic modelling of changes in the properties of KLE microcapsules over the storage period

In food science, kinetic modelling is a widely used technique to understand the changes in quality that occur during food processing. To characterize the changes in attributes (a_w , MC, TPC, TFC, TTC, DPPH, and FRAP) of KLE microcapsules over time, experimental data for these properties were fitted to proposed models using regression analysis. Fig. 5–7 provide graphical representations of the zero-order and first-order equations that describe the changes in these properties during storage. The estimated kinetic parameters for the models were determined using the regression analysis technique and are listed in Table 3.

Generally, R^2 values of both zero-order and first-order models were greater than 0.95, indicating that both models effectively describe the degradation kinetics of the studied

properties, with first-order models generally providing a slightly better fit for most properties. Previous studies have reported that both zero-order and first-order models effectively described the alterations in the quality properties over the storage period of the studied materials.^{84–86}

3.10. Prediction of the shelf life of KLE microcapsules

The period during which a product maintains its satisfactory quality before deteriorating is known as its shelf life.¹⁶ During storage, quality changes occur, leading to degradation that may limit the product's shelf life. By incorporating the reaction rate constants obtained from kinetic modelling of quality attribute changes (eqn (6)) into eqn (9), it is possible to predict the shelf life of KLE microcapsules. This equation allows for shelf-life prediction based on key quality determinants such as a_w , MC,



TPC, TFC, TTC, DPPH, and FRAP. Based on minimum moisture content and water activity, the predicted shelf-life values are detailed in Table 3. The shelf lives for the various properties of KLE microcapsules range from approximately 81 to 99 days, indicating their potential stability and longevity under the studied conditions.

4 Conclusions

This study demonstrated that spray drying offers a sustainable and scalable technique for producing kratom leaf extract (KLE) microcapsules with enhanced stability and bioactive retention. By utilizing plant-based, biodegradable wall materials—resistant maltodextrin and gum arabic—the process aligns with environmentally conscious food formulation practices. The results showed that resistant maltodextrin yielded the highest encapsulation yield and solubility, while gum arabic at 160 °C provided superior antioxidant activity retention, phenolic and flavonoid content, and encapsulation efficiency. Gum arabic, particularly at an inlet temperature of 160 °C, offers a promising formulation for preserving mitragynine and related bioactives, thereby enhancing the stability and functionality of KLE-based products. Despite slight differences in moisture content, both encapsulants retained acceptable water activity, contributing to shelf-life stability. The application of kinetic modelling further allowed prediction of microcapsule degradation during storage, with estimated shelf lives ranging from 81 to 99 days.

However, it should be noted that unequal wall material concentrations across carriers (20% GA vs. 40% RMD) may have influenced atomization, viscosity, and yield outcomes, thereby limiting the strength of direct comparisons. Future studies should validate these findings under isosolid feed conditions to ensure robust comparisons across encapsulants. Moreover, while spray drying presents promise as a practical and environmentally aligned encapsulation method, energy consumption data were not collected in this study; thus, no claims regarding “low-energy processing” can be made at this stage.

These findings support the development of sustainable functional food systems by minimizing degradation, reducing food waste, and encouraging the use of renewable, low-impact ingredients in clean-label product design.

Author contributions

Supanit Khongtongsang: investigation, formal analysis, data curation and writing – original draft. Mohammed Fikry: investigation, formal analysis, data curation and writing – original draft. Saeid Jafari: data curation and writing – original draft. Sochannet Chheng: data curation and writing – original draft. Isaya Kijpatanasilp: data curation and writing – original draft. Kitipong Assatarakul: conceptualization, data curation, funding acquisition, project administration, supervision, writing – original draft and writing – review & editing.

Conflicts of interest

The authors have no conflict of interest.

Data availability

The data supporting the findings of this study are available from the corresponding author upon request.

Acknowledgements

This study was funded by the 90th Anniversary of Chulalongkorn University Scholarship through the Ratchadapisek Somphot Endowment Fund (grant no. GCUGR1125671051M), awarded to Supanit Khongtongsang.

References

- 1 W. F. Dewatisari and E. Nuryandani, in *Proceeding International Seminar of Science and Technology*, 2025, vol. 4, pp. 49–62.
- 2 S. Charoenratana, C. Anukul and A. Aramrattana, *Int. J. Drug Policy*, 2021, **95**, 103197.
- 3 P. Sornsenee, S. Chimplee and C. Romyasamit, *Probiotics Antimicrob. Proteins*, 2023, 1–13.
- 4 C. Stanciu, S. Ahmed, S. Gnanasegaram, S. Gibson, T. Penders, O. Grundmann and C. McCurdy, *Am. J. Drug Alcohol Abuse*, 2022, **48**, 509–528.
- 5 R. Hossain, A. Sultana, M. Nuinoon, K. Noonong, J. Tangpong, K. H. Hossain and M. A. Rahman, *Molecules*, 2023, **28**, 7372.
- 6 K. Phesatcha, B. Phesatcha, M. Wanapat and A. Cherdthong, *Fermentation*, 2022, **8**, 8.
- 7 F. Zakaria, J.-K. Tan, S. M. M. Faudzi, M. B. A. Rahman and S. E. Ashari, *Ultrason. Sonochem.*, 2021, **81**, 105851.
- 8 T. Petcharat, T. Sae-leaw, S. Benjakul, T. H. Quan, S. Indriani, Y. Phimolsiripol and S. Karnjanapratum, *Process Biochem.*, 2024, **142**, 212–222.
- 9 S. Parthasarathy, J. B. Azizi, S. Ramanathan, S. Ismail, S. Sasidharan, M. I. M. Said and S. M. Mansor, *Molecules*, 2009, **14**, 3964–3974.
- 10 R. Yuniarti, S. Nadia, A. Alamanda, M. Zubir, R. Syahputra and M. Nizam, *J. Phys.: Conf. Ser.*, 2020, **1462**, 012026.
- 11 M. Çam, N. C. İçyer and F. Erdoğan, *LWT-Food Sci. Technol.*, 2014, **55**, 117–123.
- 12 E. Dobrosravić, I. Elez Garofulić, Z. Zorić, S. Pedisić, M. Roje and V. Dragović-Uzelac, *Foods*, 2023, **12**, 1923.
- 13 S. Jafari, S. M. Jafari, M. Ebrahimi, I. Kijpatanasilp and K. Assatarakul, *Food Hydrocolloids*, 2023, **134**, 108068.
- 14 S. Insang, I. Kijpatanasilp, S. Jafari and K. Assatarakul, *Ultrason. Sonochem.*, 2022, **82**, 105806.
- 15 S. Jafari, Z. Karami, K. A. Shiekh, I. Kijpatanasilp, R. W. Worobo and K. Assatarakul, *Foods*, 2023, **12**, 412.
- 16 M. Fikry, Y. A. Yusof, A. M. Al-Awaadh, R. A. Rahman and N. L. Chin, *J. Food Meas. Charact.*, 2020, **14**, 1158–1171.
- 17 D. W. Dadi, S. A. Emire, A. D. Hagos and J.-B. Eun, *Ind. Crops Prod.*, 2020, **156**, 112891.
- 18 V. Sablania, S. J. D. Bosco, S. Rohilla and M. A. Shah, *J. Food Meas. Charact.*, 2018, **12**, 892–901.
- 19 D. W. Dadi, S. A. Emire, A. D. Hagos and J.-B. Eun, *Cogent Food Agric.*, 2019, **5**, 1690316.



- 20 A. Martinić, A. Kalušević, S. Lević, V. Nedović, A. Vojvodić Cebin, S. Karlović, I. Špoljarić, G. Mršić, K. Žižek and D. Komes, *Food Technol. Biotechnol.*, 2022, **60**, 237–252.
- 21 A. Dobrinčić, L. Tuđen, M. Repajić, I. E. Garofulić, Z. Zorić, V. Dragović-Uzelac and B. Levaj, *Acta Aliment.*, 2020, **49**, 475–482.
- 22 E. González, A. M. Gómez-Caravaca, B. Giménez, R. Cebrián, M. Maqueda, A. Martínez-Férez, A. Segura-Carretero and P. Robert, *Food Chem.*, 2019, **279**, 40–48.
- 23 D. W. Dadi, S. A. Emire, A. D. Hagos and J.-B. Eun, *Ann.: Food Sci. Technol.*, 2019, **20**, 1690316.
- 24 C. Tongped and N. Trongsiriwat, Master's thesis, King Mongkut's University of Technology North Bangkok, 2025.
- 25 M. Matra, S. Phupaboon, P. Totakul, R. Prommachart, A. A. Shah, A. M. Shah and M. Wanapat, *Anim. Biosci.*, 2023, **37**, 74.
- 26 M. Matra, S. Phupaboon, P. Totakul, R. Prommachart and M. Wanapat, *Int. J. Agric. Biosci.*, 2025, **14**, 258–264.
- 27 M. Fikry, S. Jafari, K. A. Shiekh, I. Kijpatanasilp, S. Khongtongsang, E. Khojah, H. A. A. L. Jumayi and K. Assatarakul, *Ultrason. Sonochem.*, 2024, 106949, DOI: [10.1016/j.ultsonch.2024.106949](https://doi.org/10.1016/j.ultsonch.2024.106949).
- 28 M. Sharma and K. K. Dash, *Innovative Food Sci. Emerging Technol.*, 2022, **75**, 102913.
- 29 Y. Ramakrishnan, N. M. Adzahan, Y. A. Yusof and K. Muhammad, *Powder Technol.*, 2018, **328**, 406–414.
- 30 K. Slinkard and V. L. Singleton, *Am. J. Enol. Vitic.*, 1977, **28**, 49–55.
- 31 S. Chheng, M. Fikry, S. Jafari, D. K. Mishra and K. Assatarakul, *J. Stored Prod. Res.*, 2025, **112**, 102660.
- 32 M. Fikry, Y. A. Yusof, A. M. Al-Awaadh, R. A. Rahman, N. L. Chin, E. Mousa and L. S. Chang, *Food Sci. Technol. Res.*, 2019, **25**, 351–362.
- 33 M. Ahmed, M. S. Akter and J. B. Eun, *J. Sci. Food Agric.*, 2010, **90**, 494–502.
- 34 L. Wen, B. Yang, C. Cui, L. You and M. Zhao, *Food Anal. Methods*, 2012, **5**, 1244–1251.
- 35 S. Chheng and K. Assatarakul, *Summer Institute of Asia & ASEAN Center for Educational Research*, Chiba University, Japan, 2023.
- 36 K. Papoutsis, P. Pristijono, J. B. Golding, C. E. Stathopoulos, M. C. Bowyer, C. J. Scarlett and Q. V. Vuong, *J. Food Process. Preserv.*, 2017, **41**, e13152.
- 37 M. Fikry, S. Jafari, K. A. Shiekh, I. Kijpatanasilp, S. Chheng and K. Assatarakul, *Food Bioprocess Technol.*, 2024, 1–18, DOI: [10.1007/s11947-024-03421-0](https://doi.org/10.1007/s11947-024-03421-0).
- 38 S. Chheng, S. Jafari, D. Mishra and K. Assatarakul, *Sustainable Food Technol.*, 2025, **3**, 1865–1879.
- 39 P. Siddhuraju and S. Manian, *Food Chem.*, 2007, **105**, 950–958.
- 40 I. Atalar and M. Dervisoglu, *LWT-Food Sci. Technol.*, 2015, **60**, 751–757.
- 41 R. K. Cruz-Bravo, D. Guajardo-Flores, C. A. Gómez-Aldapa, J. Castro-Rosas, R. O. Navarro-Cortez, L. Díaz-Batalla and R. N. Falfán-Cortés, *CyTA-J. Food.*, 2023, **21**, 493–501.
- 42 M. Fikry, R. Sami, A. A. Al-Mushhin, A. H. Aljahani, A. Almasoudi, S. Alharthi, K. A. Ismail and M. Dabbour, *J. Biobased Mater. Bioenergy.*, 2022, **16**, 150–158.
- 43 D. Gómez-Díaz, J. M. Navaza and L. Quintáns-Riveiro, *Int. J. Food Prop.*, 2008, **11**, 773–780.
- 44 P. Pittia and M. Faieta, in *Spray Drying Encapsulation of Bioactive Materials*, CRC Press, 2021, pp. 355–376.
- 45 K. Simon-Brown, K. M. Solval, A. Chotiko, L. Alfaro, V. Reyes, C. Liu, B. Dzandu, E. Kyereh, A. G. Barnaby and I. Thompson, *LWT*, 2016, **70**, 119–125.
- 46 W. Ren, G. Tian, S. Zhao, Y. Yang, W. Gao, C. Zhao, H. Zhang, Y. Lian, F. Wang and H. Du, *Lwt*, 2020, **133**, 109954.
- 47 T. T. Tran and H. V. Nguyen, *Beverages*, 2018, **4**, 84.
- 48 C. T. Nguyen, K. N. Di, H. C. Phan, T. C. Kha and H. C. Nguyen, *Int. J. Biol. Macromol.*, 2024, **269**, 132217.
- 49 J. B. J. Tay, X. Chua, C. Ang, *et al.*, *Processes*, 2021, **9**, 1557.
- 50 T. P. Labuza and B. Altunakar, *Water Activity in Foods: Fundamentals and Applications*, 2020, pp. 161–205.
- 51 J. Astina and S. Sapwarobol, *J. Am. Coll. Nutr.*, 2019, **38**, 380–385.
- 52 O. Jordán-Suárez, J. J. Pérez-Alonso and J. J. Alvarez-Ramirez, *J. Encapsulation Adsorpt. Sci.*, 2018, **8**, 178–193.
- 53 S. Y. Quek, N. K. Chok and P. Swedlund, *Chem. Eng. Process.*, 2007, **46**, 386–392.
- 54 P. Mishra, S. Mishra and C. L. Mahanta, *Food Bioprod. Process.*, 2014, **92**, 252–258.
- 55 R. V. de Barros Fernandes, S. V. Borges and D. A. Botrel, *Carbohydr. Polym.*, 2014, **101**, 524–532.
- 56 E. J. G. Laureanti, T. S. Paiva, L. M. de Matos Jorge and R. M. M. Jorge, *Int. J. Biol. Macromol.*, 2023, **253**, 126969.
- 57 S. B. Nimse and D. Pal, *RSC Adv.*, 2015, **5**, 27986–28006.
- 58 V. M. Silva, L. E. Kurozawa, K. J. Park and M. D. Hubinger, *Drying Technol.*, 2012, **30**, 175–184.
- 59 C. Cao, X. Zhao, C. Zhang, Z. Ding, F. Sun and C. Zhao, *J. Food Sci.*, 2020, **85**, 3442–3449.
- 60 E. M. Mudge and P. N. Brown, *J. AOAC Int.*, 2017, **100**, 18–24.
- 61 N. Isnaeni, A. Saefumillah and A. H. Cahyana, *Indones. J. Food Drug Saf.*, 2024, **4**, 130–144.
- 62 A. Al-Hamayda, B. Abu-Jdayil, M. Ayyash and J. Tannous, *Ind. Crops Prod.*, 2023, **205**, 117556.
- 63 E. Díaz-Montes, *Polymers*, 2023, **15**, 2659.
- 64 D. A. Pai, V. R. Vangala, J. W. Ng, W. K. Ng and R. B. Tan, *J. Food Eng.*, 2015, **161**, 68–74.
- 65 H. C. Carneiro, R. V. Tonon, C. R. Grosso and M. D. Hubinger, *J. Food Eng.*, 2013, **115**, 443–451.
- 66 A. Tolun, Z. Altintas and N. Artik, *J. Biotechnol.*, 2016, **239**, 23–33.
- 67 L. Alamilla-Beltran, J. J. Chanona-Perez, A. R. Jimenez-Aparicio and G. F. Gutierrez-Lopez, *J. Food Eng.*, 2005, **67**, 179–184.
- 68 Z. Zhang, S. Zhang, R. Su, D. Xiong, W. Feng and J. Chen, *J. Food Sci.*, 2019, **84**, 1427–1438.
- 69 R. Vehring, H. Snyder and D. Lechuga-Ballesteros, *Drying Technol. Biotechnol. Pharm. Appl.*, 2020, 179–216.
- 70 R. Chedoloh and S.-A. Asae, *Burapha Sci. J.*, 2017, 78–91.
- 71 A. Dutta and G. Dutta, *J. Appl. Packag. Res.*, 2016, **8**, 5.
- 72 S. N. Dirim and G. Çalıřkan, *J. Food*, 2012, **37**(4), 203–210.



- 73 C. Wong and W. Lim, *Int. Food Res. J.*, 2016, **23**, 1887.
- 74 O. Jiménez-González and J. Á. Guerrero-Beltrán, *Food Eng. Rev.*, 2021, **13**, 769–811.
- 75 S. C. de Moura, C. L. Berling, A. O. Garcia, M. B. Queiroz, I. D. Alvim and M. D. Hubinger, *Food Res. Int.*, 2019, **121**, 542–552.
- 76 R. V. Tonon, C. Brabet and M. D. Hubinger, *J. Food Eng.*, 2008, **88**, 411–418.
- 77 J. K. Agbenorhevi and L. J. Marshall, *J. Food Sci. Eng.*, 2012, **2**, 72.
- 78 S. Agustini and M. K. Yusya, *Curr. Res. Biosci. Biotechnol.*, 2020, **1**, 66–70.
- 79 C. Baltacıoğlu, S. Velioglu and E. Karacabey, *J. Food Qual.*, 2011, **34**, 278–283.
- 80 M. Thakur and V. Nanda, *Food Chem. Adv.*, 2024, **4**, 100567.
- 81 S. Warnasih and U. Hasanah, *J. Sci. Innovare*, 2019, **1**, 44–49.
- 82 T. Okuda and H. Ito, *Molecules*, 2011, **16**, 2191–2217.
- 83 K. Jitrangsri, A. Chaidedgumjorn and M. Satiraphan, *Pharm. Sci. Asia*, 2020, **47**, 164–172.
- 84 S. C. Foo, F. M. Yusoff and N. M. Khong, *J. Agric. Food Res.*, 2024, **15**, 100823.
- 85 C. Bustos-Garza, J. Yáñez-Fernández and B. E. Barragán-Huerta, *Food Res. Int.*, 2013, **54**, 641–649.
- 86 S. A. Desobry, F. M. Netto and T. P. Labuza, *J. Food Sci.*, 1997, **62**, 1158–1162.

